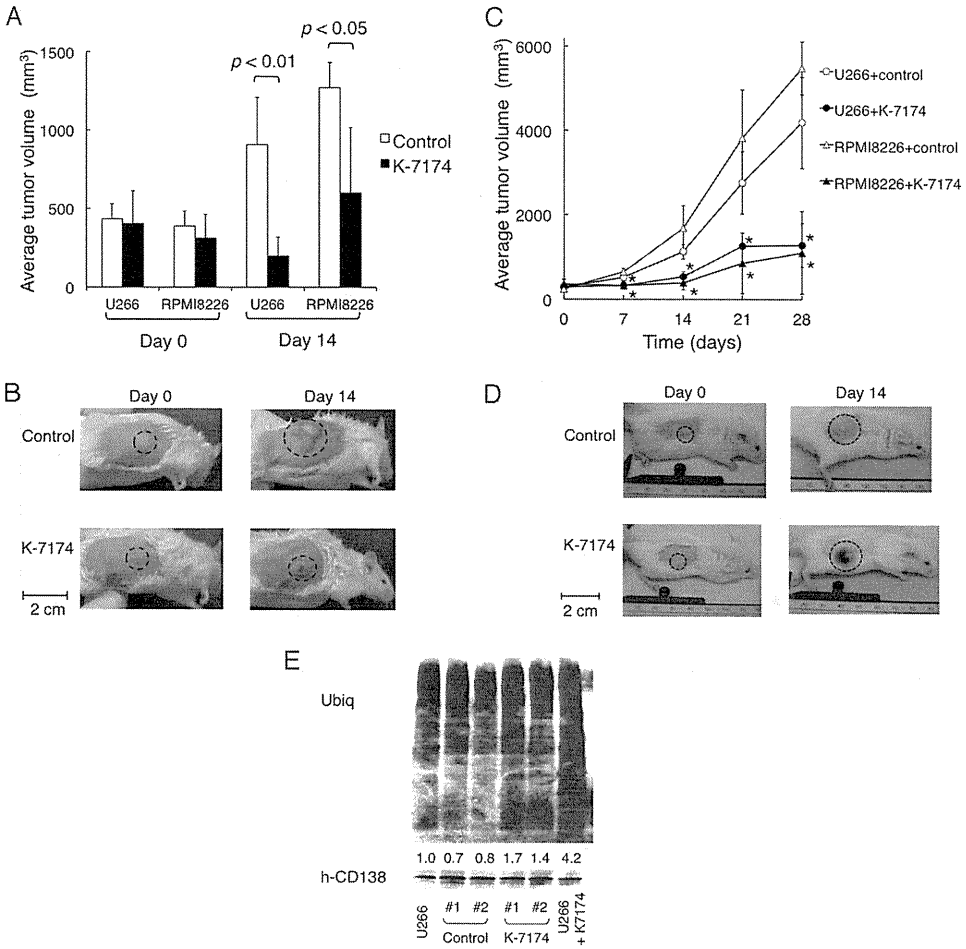

FIGURE 2. **Anti-myeloma activity of K-7174 *in vivo*.** NOD/SCID mice were inoculated subcutaneously with 1×10^7 cells of U266 or 3×10^7 cells of RPMI8226 into the right thigh. Treatments were started on day 0, when tumors were measurable. Caliper measurements of the longest perpendicular tumor diameters were performed on alternate days to estimate the tumor volume (mm^3) using the following formula: $4/3\pi \times (\text{width}/2)^2 \times (\text{length}/2)$. *A*, mice were treated with 75 mg/kg of K-7174 intraperitoneally once daily for 14 days ($n = 4$) or the vehicle (3% DMSO in 0.9% NaCl) alone (*Control*) on the same schedule ($n = 4$). The *y* axis shows the average tumor volume in inoculated mice on the indicated days. The mean ± S.D. (*bars*) are shown. *p* values were calculated by one-way analysis of variance with the Student-Newman-Keuls multiple comparisons test. *B*, representative photographs of NOD/SCID mice inoculated with U266 cells on days 0 and 14 (original magnification: ×2). Inoculated tumors are indicated in *circled* regions. *C*, mice were treated with 50 mg/kg of K-7174 post-orally once daily for 14 days (U266 + K-7174, *closed circle*; $n = 3$, RPMI8226 + K-7174, *closed triangle*; $n = 3$), or the vehicle (3% DMSO in 0.9% NaCl) alone on the same schedule (U266 + control, *open circle*; $n = 4$, RPMI8226 + control, *open triangle*; $n = 3$). The *y* axis shows the average tumor volume in inoculated mice (*bars* indicate S.D.). *p* values were calculated by one-way analysis of variance with the Student-Newman-Keuls multiple comparisons test. *Asterisks* indicate $p < 0.05$ against the vehicle control. *D*, representative photographs of NOD/SCID mice inoculated with RPMI8226 cells on days 0 and 14 (original magnification: ×2). Inoculated tumors are indicated in *circled* regions. *E*, NOD/SCID mice were inoculated subcutaneously with 1×10^7 cells of U266 into the right thigh. When tumors were measurable, mice were treated with 50 mg/kg of K-7174 post-orally once daily (K-7174; $n = 2$) or the vehicle (3% DMSO in 0.9% NaCl) alone (Control; $n = 2$) for 3 days. We resected inoculated tumors and sorted human CD138-positive cells using a FACSaria flow cytometer for immunoblot analysis of cellular protein ubiquitination (*Ubiq*) and CD138 (*hCD38*) expression. We used lysates of U266 cells treated with 5 μM K-7174 (U266 + K-7174) or the vehicle control (*U266*) for 3 days *in vitro* as controls. The signal intensities were quantified by densitometry, normalized to those of the corresponding CD138, and shown as relative values setting the vehicle control (*U266*) to 1.0.

TABLE 1

Biochemical parameters of mice treated with K-7174

We evaluated the indicated parameters in mice on day 21 of K-7174 treatment. Data are shown as the mean ± S.D. ($n = 3$ per group). *p* values were calculated by the Student's *t* test.

	Vehicle	K-7174 (50 mg/kg)	*p* value
Body weight (g)	23.0 ± 0.9	27.8 ± 0.7	$p > 0.05$
Peripheral blood count			
WBC ($\times 10^2/\mu l$)	28.8 ± 1.6	27.5 ± 1.3	$p > 0.05$
RBC ($\times 10^4/\mu l$)	653.3 ± 90.2	694.8 ± 24.9	$p > 0.05$
HGB (g/dl)	10.9 ± 1.5	11.6 ± 0.5	$p > 0.05$
HCT (%)	32.6 ± 4.4	34.8 ± 1.7	$p > 0.05$
MCV (fl)	49.9 ± 0.4	50.1 ± 0.9	$p > 0.05$
Mean corpuscular hemoglobin (pg)	16.6 ± 0.1	16.6 ± 0.4	$p > 0.05$
Mean corpuscular hemoglobin concentration (g/dl)	33.3 ± 0.1	33.2 ± 0.2	$p > 0.05$
Platelet ($\times 10^4/\mu l$)	35.8 ± 9.7	26.5 ± 15.6	$p > 0.05$
Serum level			
Aspartate aminotransferase (units/liter)	113.8 ± 32.1	74.8 ± 10.0	$p > 0.05$
Alanine aminotransferase (units/liter)	8.8 ± 2.8	10.3 ± 2.6	$p > 0.05$

lated with not only the WT subline (Fig. 3*B*, *left panel*) but also the mutant subline (Fig. 3*B*, *right panel*), indicating that K-7174 overcomes mutant *PSMB5*-confered bortezomib resistance *in vivo*.

Furthermore, we examined the effects of K-7174 on primary MM cells isolated from a patient who was heavily treated and became resistant to bortezomib. CD138-positive bone marrow mononuclear cells were cultured in the absence or presence of either K-7174 or bortezomib for 2 days, followed by annexin-V staining. Primary MM cells from 2 untreated patients were used as controls. Bortezomib induced apoptosis in control MM cells in a dose-dependent manner, but not in cells from a bortezomib-resistant patient (Fig. 3*C*, *right panel*). In contrast, K-7174 was able to induce apoptosis in primary MM cells from a bortezomib-resistant patient as well as untreated patients,

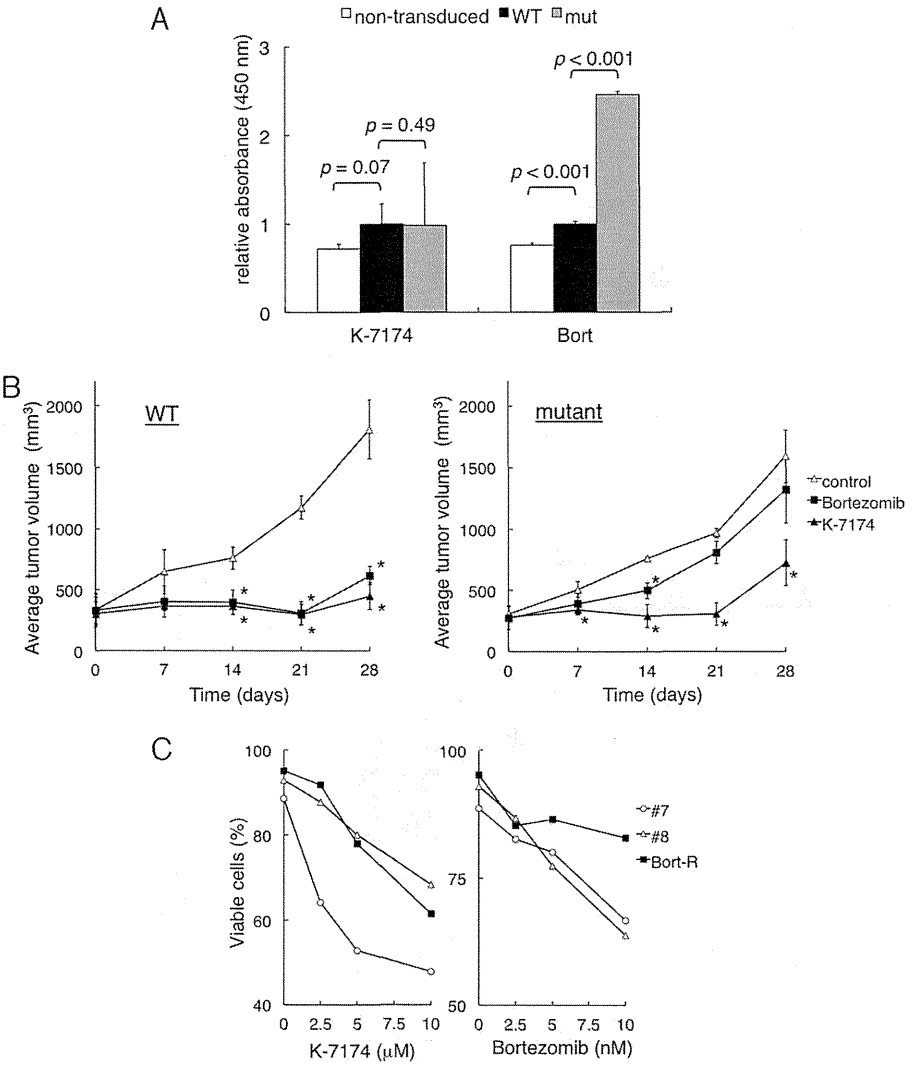

FIGURE 3. **Cytotoxic effects of K-7174 on bortezomib-resistant MM cells.** We established wild-type (WT) and mutant (*mut*) sublines from RPMI8226 by transducing with wild-type and mutated *PSMB5* cDNA, respectively. *A*, cell proliferation was measured by MTT assays after culturing non-transduced cells and each subline with either K-7174 or bortezomib for 72 h. The *y* axis shows the relative absorbance setting wild-type values to 1.0. *p* values were calculated by one-way analysis of variance with the Student-Newman-Keuls multiple comparisons test. *B*, NOD/SCID mice were inoculated subcutaneously with 1×10^7 cells of wild-type (WT) or mutant (*mutant*) subline into the right thigh. Mice were treated with the vehicle (3% DMSO in 0.9% NaCl) alone (control, *open triangle*; $n = 3$), bortezomib, 0.5 mg/kg, intravenously twice a week (Bortezomib, *closed square*; $n = 4$), or K-7174, 50 mg/kg, post-orally once daily (K-7174, *closed triangle*; $n = 4$), respectively, for 2 weeks. The *y* axis shows the average tumor volume in inoculated mice (*bars* indicate S.D.). *p* values were calculated by one-way analysis of variance with the Student-Newman-Keuls multiple comparisons test. *Asterisks* indicate $p < 0.05$ against the vehicle control. *C*, primary MM cells were cultured with either K-7174 or bortezomib at the indicated doses for 48 h. Cell death/apoptosis was determined by reactivity with annexin-V on a flow cytometer. The *y* axis shows the proportion of annexin-V-positive cells (%).

although there was a variation in drug sensitivity (Fig. 3*C*, *left panel*). These results imply that K-7174 has a potential to overcome bortezomib resistance clinically.

Class I HDACs Are Critical Targets of K-7174-induced Cytotoxicity in MM Cells—We have previously shown that bortezomib treatment results in transcriptional repression of class I HDACs, which plays a critical role in bortezomib-mediated cytotoxicity in MM cells (21). We investigated whether this is the case with K-7174. To this end, we examined the expression of class I HDACs (HDAC1, -2, and -3) in MM cell lines during K-7174 treatment. Immunoblot analyses revealed that K-7174 down-regulated HDAC1 expression and reciprocally induced histone hyperacetylation in a dose- and time-dependent fashion (Fig. 4, *A* and *B*). To determine whether the down-regulation of HDAC expression occurred at transcriptional or post-transcriptional levels, we performed semi-quantitative RT-PCR analyses. As a result, K-7174 down-regulated *class I HDAC* genes (*HDAC1*, *-2*, and *-3*) at mRNA levels in all three MM cell lines in a time-dependent fashion (Fig. 4*C*). In addition, there were no significant changes in the expression of *class II* and *III HDAC* genes such as *HDAC4*, *-5*, *-6*, and *SIRT1* during K-7174 treatment (Fig. 4*D*). K-7174 also decreased the expression levels of *class I HDAC* genes (HDAC1, -2, and -3) in CD138-positive cells isolated from the bone marrow of four MM patients (Fig. 4*E*). These results suggest that K-7174 specifically repressed the transcription of *class I HDACs* in MM cells.

To confirm the dependence of K-7174 action on class I HDAC expression, we performed gain-of-function of HDAC1, -2, and -3 using the lentiviral transduction system as described previously (21). Overexpression of each class I

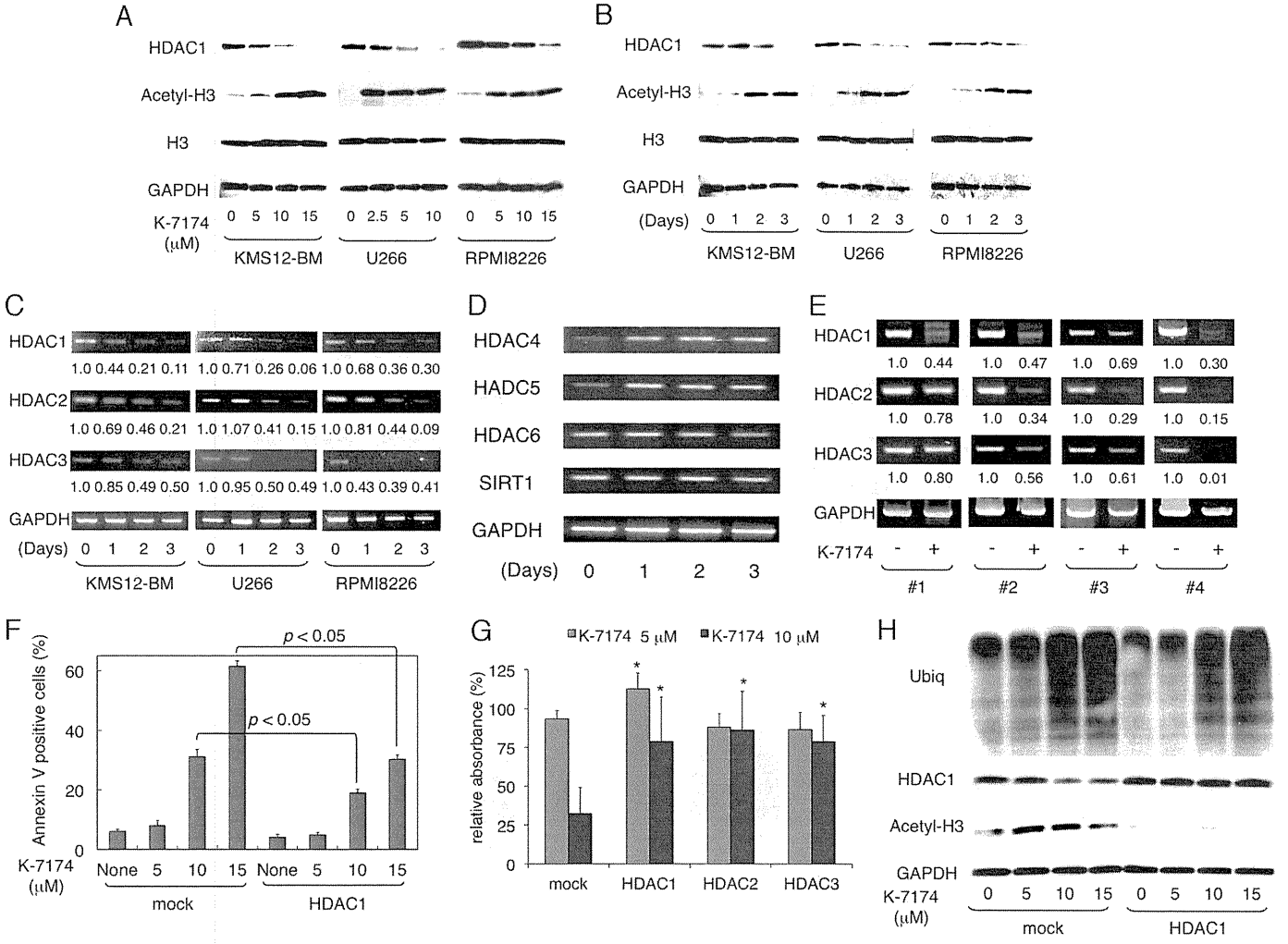

FIGURE 4. **Cytotoxic effects of K-7174 depends on the expression levels of class I HDACs in MM cells.** *A*, MM cell lines (KMS12-BM, U266, and RPMI8226) were cultured with K-7174 at the indicated doses for 48 h. Whole cell lysates were subjected to immunoblotting for the expression of HDAC1, acetylated histone H3, histone H3, and GAPDH (internal control). *B*, MM cell lines were cultured with K-7174 (5 μM for U266 and 10 μM for KMS12-BM and RPMI8226) for up to 3 days. Whole cell lysates were prepared at the given time points and subjected to immunoblotting as described above. *C*, total cellular RNA was isolated simultaneously in the experiments described in *panel B* and subjected to semi-quantitative RT-PCR analysis for the expression of *HDAC1*, *HDAC2*, *HDAC3*, and *GAPDH* (internal control). The amplified products were visualized by ethidium bromide staining after 2% agarose gel electrophoresis. The results of suboptimal amplification cycles, 35 cycles, are shown. The signal intensities of each band were quantified, normalized to those of the corresponding *GAPDH*, and shown as relative values setting Day 0 controls to 1.0. *D*, total cellular RNA was isolated from RPMI8226 cells in the experiments described in *panel B* and subjected to semi-quantitative RT-PCR analysis for the expression of *HDAC4*, *HDAC5*, *HDAC6*, *SIRT1*, and *GAPDH* (internal control). The amplified products were visualized by ethidium bromide staining after 2% agarose gel electrophoresis. The results of suboptimal amplification cycles (35 cycles) are shown. Detailed information of primers, including sequences, corresponding nucleotide positions and PCR product sizes, was described previously (21). *E*, we cultured primary MM cells with either 10 μM K-7174 (+) or the vehicle alone (−) for 48 h. The mRNA expression of class I HDACs was examined by RT-PCR as described above. *F*, RPMI8226 cells were transduced with either CSII-DsRed (*mock*) or CSII-DsRed-HDAC1 (*HDAC1*) vector as described previously (21). Transduced cells were cultured in the absence or presence of 5, 10, and 15 μM K-7174 for 48 h. Cells were harvested, stained with annexin-V, and subjected to flow cytometric analysis. The *y* axis shows the proportion of annexin-V positivity in the DsRed-positive fraction. The mean ± S.D. (*bars*) of three independent experiments are shown. *p* values were calculated by one-way analysis of variance with Student-Newman-Keuls multiple comparisons test. *G*, RPMI8226 cells were transduced with CSII-DsRed (*mock*), CSII-DsRed-HDAC1 (*HDAC1*), CSII-DsRed-HDAC2 (*HDAC2*), and CSII-DsRed-HDAC3 (*HDAC3*) vectors as described previously (21). Cell proliferation was measured by MTT assays after culture in the absence or presence of 5 and 10 μM K-7174 for 72 h. The *y* axis shows a percentage of the value of corresponding to untreated cells. The mean ± S.D. (*bars*) of three independent experiments are shown. *p* values were calculated by one-way analysis of variance with the Student-Newman-Keuls multiple comparisons test. *Asterisks* indicate $p < 0.05$ against the mock. *H*, whole cell lysates were prepared simultaneously in the experiments described in *panel E* and subjected to immunoblotting for the expression of ubiquitinated proteins (*Ubiq*), HDAC1, acetylated histone H3, and GAPDH (internal control).

HDAC member significantly ameliorated K-7174-induced apoptosis in RPMI8226 cells (Fig. 4, *F* and *G*). In addition, we examined the status of histone acetylation in these cells. As anticipated, HDAC1 overexpression almost completely abrogated K-7174-induced histone hyperacetylation without affecting the accumulation of ubiquitinated proteins (Fig. 4*H*). Taken together, these results indicate that the anti-myeloma action of K-7174 is mediated via proteasome inhibition and subsequent transcriptional repression of class I HDACs.

K-7174 Induces Transcriptional Repression of Class I HDAC Genes via Caspase-8-mediated Degradation of Sp1—Next, we investigated the mechanisms of the transcriptional repression of *class I HDAC* genes by K-7174. We have previously demonstrated that Sp1 and GATA1 are major transcriptional activators of *class I HDAC* genes (28); however, MM cells barely expressed GATA transcription factors (data not shown). We therefore focused on the role of Sp1 in K-7174-induced down-regulation of *HDAC* gene expression (28, 29). To determine the

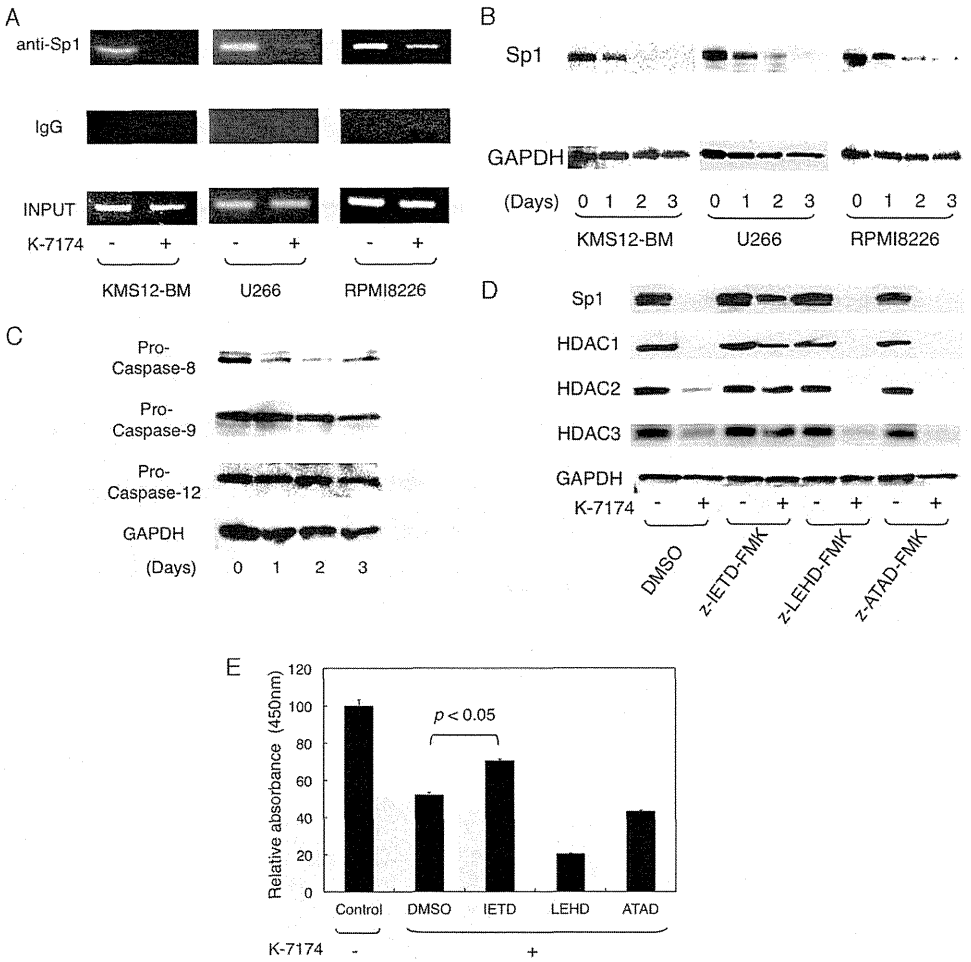

FIGURE 5. **K-7174 induces transcriptional repression of class I HDAC genes via caspase-8-mediated degradation of Sp1.** *A*, MM cell lines were cultured with either K-7174 (+) or vehicle control (−) for 2 days, and subjected to chromatin immunoprecipitation assays. Chromatin suspensions were immunoprecipitated with anti-Sp1 and isotype-matched (IgG) antibodies. The resulting precipitants were subjected to PCR to amplify the promoter regions of the *HDAC1* gene as described previously (21). The amplified products were visualized by ethidium bromide staining after 2% agarose gel electrophoresis. Representative data of 50 cycles are shown. *Input* indicates that PCR was performed with genomic DNA. *B*, MM cell lines were cultured with K-7174 (5 μM for U266 and 10 μM for KMS12-BM and RPMI8226) for up to 3 days. Whole cell lysates were prepared at the given time points and subjected to immunoblotting for Sp1 and GAPDH (internal control). *C*, RPMI8226 cells were cultured with 10 μM K-7174 for up to 3 days. Whole cell lysates were subjected to immunoblotting for pro-caspase-8, -9, and -12 and GAPDH (internal control). *D*, RPMI8226 cells were cultured with 100 μM Z-IETD-fmk (caspase-8 inhibitor), 100 μM Z-LEHD-fmk (caspase-9 inhibitor), 20 μM Z-ATAD-fmk (caspase-12 inhibitor), or vehicle alone (DMSO) for 48 h in the absence or presence of 10 μM K-7174. Whole cell lysates were subjected to immunoblotting for Sp1, HDAC1, HDAC2, HDAC3, and GAPDH (internal control). *E*, cell viability was determined after culturing RPMI8226 cells in the absence (*Control*) or presence of 10 μM K-7174 with 100 μM Z-IETD-fmk (*IETD*), 100 μM Z-LEHD-fmk (*LEHD*), 20 μM Z-ATAD-fmk (*ATAD*), or the vehicle control (DMSO) for 72 h. Absorbance at 450 nm was measured with a microplate reader, and expressed as a percentage of the value of the corresponding control cells. The mean ± S.D. (*bars*) of three independent experiments are shown. *p* values were calculated by one-way analysis of variance with the Student-Newman-Keuls multiple comparisons test.

binding of Sp1 to the promoter region of the *HDAC1* gene, we performed chromatin immunoprecipitation assays. Sp1 was bound in the *HDAC1* promoter regions of untreated MM cells, but dissociated from the promoter upon K-7174 treatment (Fig. 5*A*). These results suggest that K-7174 targets Sp1 but not GATA1 in MM cells, prompting us to examine the expression of Sp1 during K-7174 treatment. K-7174 markedly diminished the expression levels of Sp1 protein in all three MM cell lines in a time-dependent fashion (Fig. 5*B*), whereas *Sp1* mRNA levels were unchanged (data not shown). To investigate the mechanisms of the decrease in Sp1 protein levels, we determined the activation of caspases in K-7174-treated MM cells, because the Sp1 protein is degraded by caspase-8 during bortezomib treatment (21). Immunoblot analyses revealed that K-7174 activated caspase-8 but not caspase-9 and -12 (Fig. 5*C*). The peptide inhibitor of caspase-8 (Z-IETD-fmk), but not caspase-9 (Z-LETD-fmk) and caspase-12 (Z-ATAD-fmk), was able to abrogate K-7174-induced down-regulation of *Sp1*, *HDAC1*, *HDAC2*, and *HDAC3* (Fig. 5*D*) as well as cytotoxicity in RPMI8226 cells (Fig. 5*E*). These results suggest that K-7174 degraded Sp1 protein via the caspase-8-dependent pathway, leading in turn to transcriptional repression of *class I HDAC* genes in MM cells.

Combination of K-7174 and HDAC Inhibitors Exerts Additive Cytotoxic Effects on MM Cells—Finally, we examined the combined effects of K-7174 and other therapeutic agents on MM. Isobologram analyses revealed that K-7174 showed additive cytotoxicity with HDAC inhibitors (romidepsin and vorinostat) in RPMI8226 cells, whereas no such effect was observed in combination with alkylating agents (cyclophosphamide and melphalan) (Fig. 6*A*). To understand the molecular mechanisms of the additive effects, we examined the expression of

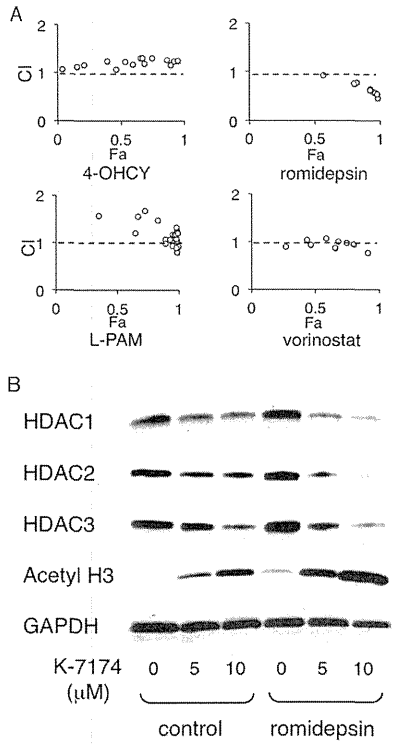

FIGURE 6. **Additive cytotoxic effects of K-7174 and HDAC inhibitors.** *A*, we cultured RPMI8226 cells with various concentrations of K-7174 in combination with 4-hydroperoxy cyclophosphamide (*4-OHCY*), melphalan (L-*PAM*), romidepsin, or vorinostat, and assessed for the cell viability after 72 h. Isobologram analysis was carried out using the CompuSyn software program to obtain the combination index (*CI*). The CI values of less than 1.0 and greater than 1.0 indicate synergism and antagonism, respectively, by definition (44). *B*, whole cell lysates were prepared simultaneously in the experiments described in *panel A* and subjected to immunoblotting for the expression of HDAC1, HDAC2, HDAC3, acetylated histone H3, and GAPDH (internal control).

class I HDACs by immunoblotting and determined the cellular HDAC activity by monitoring the status of histone acetylation. Romidepsin markedly enhanced K-7174-induced hyperacetylation of histone H3 in RPMI8226 cells (Fig. 6*B*). These results suggest that class I HDACs are critical molecular targets of K-7174, and HDAC inhibitors may be helpful in enhancing therapeutic effects of K-7174.

DISCUSSION

In the present study, we show that (i) K-7174 is a novel orally active PI, which exhibits *in vitro* and *in vivo* cytotoxicity against MM cells, (ii) is more effective with oral administration than intraperitoneal injection in a murine xenograft model, (iii) is effective for bortezomib-resistant MM cell lines and primary MM cells, (iv) targets class I HDACs for cytotoxicity, and (v) induces additive effects with HDAC inhibitors. This is the first report demonstrating a model system to show that bortezomib resistance could be overcome by a PI and the critical role of class I HDACs in PI-induced cytotoxicity other than bortezomib. Taken together, K-7174 could be a novel therapeutic agent for MM, which allows for flexibility in the dosing schedule, increased patient convenience, and overcoming bortezomib resistance. In addition, K-7174 may be combined with other orally active anti-myeloma agents, such as lenalidomide and vorinostat, to establish the post-oral regimens suitable for treatment in the outpatient clinic.

K-7174 was originally reported as a specific inhibitor of GATA family transcription factors. Umetani *et al.* (16) reported that K-7174 inhibited cell adhesion via the down-regulation of vascular cell adhesion molecule-1 (VCAM-1) expression on endothelial cells. VCAM-1 is known to be a ligand for very late antigen-4, which was identified as a key molecule for cell adhesion-mediated drug resistance in MM cells (24); therefore, K-7174 may inhibit cell adhesion between stromal cells and MM cells and overcome drug resistance. In addition, Imagawa *et al.* (17) demonstrated that injection of K-7174 restored erythropoietin production and improved anemia of chronic disease in an *in vivo* mouse assay. As severe anemia is frequently observed in MM patients, K-7174 is also expected to improve anemia associated with MM.

Previous studies showed that the unfolded protein response is a major mechanism of anti-myeloma action of bortezomib (30); however, our studies indicate a critical role of class I HDACs in K-7174- and bortezomib-induced cytotoxicity (21). Their expressions were down-regulated at a transcriptional level via caspase-8-dependent degradation of the Sp1 protein. As a result, class I HDAC activity was reduced, leading to cytotoxicity in MM cells. We have also demonstrated that the caspase-12 inhibitor, which could inhibit ER stress-induced apoptosis, did not affect K-7174- and bortezomib-induced apoptosis but the caspase-8 inhibitor did. The caspase-8-mediated pathway is dominant over the unfolded protein response in our system. Supporting this idea, Mannava *et al.* (31) have recently reported that KLF9, which is indirectly transactivated by bortezomib, determines the response to bortezomib independently of the induction of ER stress. They have also shown that bortezomib-induced apoptosis largely depends on the class I HDAC activity. Moreover, Miller *et al.* (32) reported that caspase-8-dependent histone acetylation is essential for apoptosis induced by NPI-0052, a novel PI under preclinical investigation, in leukemia cells. Taken together, it appears that class I HDACs are critical targets of PI-induced cytotoxicity in hematological malignancies in general. However, the involvement of other mechanisms cannot be ruled out, because HDAC1 overexpression only partially ameliorated K-7174-induced apoptosis. Further investigation is required to fully elucidate the underlying mechanisms of K-7174 action in MM cells.

Although these findings indicate class I HDACs as valid therapeutic targets for MM, HDAC inhibitors, such as vorinostat and romidepsin, showed limited efficacy as single agents in clinical trials (33, 34). This may be attributable to the fact that the class I HDACs mediate various cellular events via not only deacetylation of core histones but also association with various non-histone proteins, causing a variety of side effects (35–37). The combination with PIs might be a strategy to overcome the limitation. On the other hand, HDAC inhibitors have attracted attention for their ability in restoring drug sensitivity in gefitinib-tolerant non-small cell lung cancer (38) and BCR-ABL-positive imatinib-resistant chronic myeloid leukemia stem cells (39). We have also shown that the HDAC inhibitor romidepsin could overcome bortezomib resistance conferred by HDAC1 overexpression in a murine xenograft model (21). Recently, Chesi *et al.* (40) demonstrated that the combination of HDAC inhibitors, vorinostat and panobinostat, with bort-

ezomib would be effective in the treatment of relapsed MM using genetically engineered mouse models. These results suggest that HDAC inhibitors are effective in overcoming intrinsic drug resistance of malignant cells. Indeed, Harrison *et al.* (41) and Knop (42) have reported the successful results of clinical trials with romidepsin and bortezomib/dexamethasone for relapsed and/or refractory MM. These pre-clinical and clinical studies suggest that class I HDACs are effective therapeutic targets and the combination of PIs with HDAC inhibitors may represent the best treatment strategy for MM patients (21, 43).

Acknowledgments—We are grateful to Drs. Hiroaki Kimura and Naoya Shibayama (Jichi Medical School) for helpful discussions and technical advice and Akiko Yonekura for excellent assistance.

REFERENCES

1. Moreau, P., Richardson, P. G., Cavo, M., Orlowski, R. Z., San Miguel, J. F., Palumbo, A., and Harousseau, J. L. (2012) Proteasome inhibitors in multiple myeloma. 10 years later. *Blood* **120,** 947–959
2. Friedberg, J. W., Vose, J. M., Kelly, J. L., Young F., Bernstein, S. H., Peterson, D., Rich, L., Blumel, S., Proia, N. K., Liesveld, J., Fisher, R. I., Armitage, J. O., Grant, S., and Leonard, J. P. (2011) The combination of bendamustine, bortezomib, and rituximab for patients with relapsed/refractory indolent and mantle cell non-Hodgkin lymphoma. *Blood* **117,** 2807–2812
3. San Miguel, J. F., Schlag, R., Khuageva, N. K., Dimopoulos, M. A., Shpilberg, O., Kropff, M., Spicka, I., Petrucci, M. T., Palumbo, A., Samoilova, O. S., Dmoszynska, A., Abdulkadyrov, K. M., Delforge, M., Jiang, B., Mateos, M. V., Anderson, K. C., Esseltine, D. L., Liu, K., Deraedt, W., Cakana, A., van de Velde, H., and Richardson, P. G. (2013) Persistent overall survival benefit and no increased risk of second malignancies with bortezomib-melphalan-prednisone *versus* melphalan-prednisone in patients with previously untreated multiple myeloma. *J. Clin. Oncol.* **31,** 448–455
4. Lonial, S., Waller, E. K., Richardson, P. G., Jagannath, S., Orlowski, R. Z., Giver, C. R., Jaye, D. L., Francis, D., Giusti, S., Torre, C., Barlogie, B., Berenson, J. R., Singhal, S., Schenkein, D. P., Esseltine, D. L., Anderson, J., Xiao, H., Heffner, L. T., and Anderson, K. C., SUMMIT/CREST Investigators. (2005) Risk factors and kinetics of thrombocytopenia associated with bortezomib for relapsed, refractory multiple myeloma. *Blood* **106,** 3777–3784
5. Richardson, P. G., Briemberg, H., Jagannath, S., Wen, P. Y., Barlogie, B., Berenson, J., Singhal, S., Siegel, D. S., Irwin, D., Schuster, M., Srkalovic, G., Alexanian, R., Rajkumar, S. V., Limentani, S., Alsina, M., Orlowski, R. Z., Najarian, K., Esseltine, D., Anderson, K. C., and Amato, A. A. (2006) Frequency, characteristics, and reversibility of peripheral neuropathy during treatment of advanced multiple myeloma with bortezomib. *J. Clin. Oncol.* **24,** 3113–3120
6. Hideshima, T., and Anderson, K. C. (2011) Novel therapies in MM. From the aspect of preclinical studies. *Int. J. Hematol.* **94,** 344–354
7. Kuhn, D. J., Chen, Q., Voorhees, P. M., Strader, J. S., Shenk, K. D., Sun, C. M., Demo, S. D., Bennett, M. K., van Leeuwen, F. W., Chanan-Khan, A. A., and Orlowski, R. Z. (2007) Potent activity of carfilzomib, a novel, irreversible inhibitor of the ubiquitin-proteasome pathway, against preclinical models of multiple myeloma. *Blood* **110,** 3281–3290
8. Khan, M. L, and Stewart, A. K. (2011) Carfilzomib. A novel second-generation proteasome inhibitor. *Future Oncol.* **7,** 607–612
9. Chauhan, D., Catley, L., Li, G., Podar, K., Hideshima, T., Velankar, M., Mitsiades, C., Mitsiades, N., Yasui, H., Letai, A., Ovaa, H., Berkers, C., Nicholson, B., Chao, T. H., Neuteboom, S. T., Richardson, P., Palladino, M. A., and Anderson, K. C. (2005) A novel orally active proteasome inhibitor induces apoptosis in multiple myeloma cells with mechanisms distinct from Bortezomib. *Cancer Cell* **8,** 407–419
10. Piva, R., Ruggeri, B., Williams, M., Costa, G., Tamagno, I., Ferrero, D., Giai, V., Coscia, M., Peola, S., Massaia, M., Pezzoni, G., Allievi, C., Pescalli, N., Cassin, M., di Giovine, S., Nicoli, P., de Feudis, P., Strepponi, I., Roato, I., Ferracini, R., Bussolati, B., Camussi, G., Jones-Bolin, S., Hunter, K., Zhao, H., Neri, A., Palumbo, A., Berkers, C., Ovaa, H., Bernareggi, A., and Inghirami, G. (2008) CEP-18770. A novel, orally active proteasome inhibitor with a tumor-selective pharmacologic profile competitive with bortezomib. *Blood* **111,** 2765–2775
11. Kupperman, E., Lee, E. C., Cao, Y., Bannerman, B., Fitzgerald, M., Berger, A., Yu, J., Yang, Y., Hales, P., Bruzzese, F., Liu, J., Blank, J., Garcia, K., Tsu, C., Dick, L., Fleming, P., Yu, L., Manfredi, M., Rolfe, M., and Bolen, J. (2010) Evaluation of the proteasome inhibitor MLN9708 in preclinical models of human cancer. *Cancer Res.* **70,** 1970–1980
12. Chauhan, D., Singh, A. V., Aujay, M., Kirk, C. J., Bandi, M., Ciccarelli, B., Raje, N., Richardson, P., and Anderson, K. C. (2010) A novel orally active proteasome inhibitor ONX 0912 triggers *in vitro* and *in vivo* cytotoxicity in multiple myeloma. *Blood* **116,** 4906–4915
13. Lü, S., Yang, J., Song, X., Gong, S., Zhou, H., Guo, L., Song, N., Bao, X., Chen, P., and Wang, J. (2008) Point mutation of the proteasome β5 subunit gene is an important mechanism of bortezomib resistance in bortezomib-selected variants of Jurkat T cell lymphoblastic lymphoma/leukemia line. *J. Pharmacol. Exp. Ther.* **326,** 423–431
14. Oerlemans, R., Franke, N. E., Assaraf, Y. G., Cloos, J., van Zantwijk, I., Berkers, C. R., Scheffer, G. L., Debipersad, K., Vojtekova, K., Lemos, C., van der Heijden, J. W., Ylstra, B., Peters, G. J., Kaspers, G. L., Dijkmans, B. A., Scheper, R. J., and Jansen, G. (2008) Molecular basis of bortezomib resistance. Proteasome subunit β5 (PSMB5) gene mutation and over-expression of PSMB5 protein. *Blood* **112,** 2489–2499
15. Franke, N. E., Niewerth, D., Assaraf, Y. G., van Meerloo, J., Vojtekova, K., van Zantwijk, C. H., Zweegman, S., Chan, E. T., Kirk, C. J., Geerke, D. P., Schimmer, A. D., Kaspers, G. J., Jansen, G., and Cloos, J. (2012) Impaired bortezomib binding to mutant β5 subunit of the proteasome is the underlying basis for bortezomib resistance in leukemia cells. *Leukemia* **26,** 757–768
16. Umetani, M., Nakao, H., Doi, T., Iwasaki, A., Ohtaka, M., Nagoya, T., Mataki, C., Hamakubo, T., and Kodama, T. (2000) A novel cell adhesion inhibitor, K-7174, reduces the endothelial VCAM-1 induction by inflammatory cytokines, acting through the regulation of GATA. *Biochem. Biophys. Res. Commun.* **272,** 370–374
17. Imagawa, S., Nakano, Y., Obara, N., Suzuki, N., Doi, T., Kodama, T., Nagasawa, T., and Yamamoto, M. (2003) A GATA-specific inhibitor (K-7174) rescues anemia induced by IL-1β, TNF-α, or L-NMMA. *FASEB J.* **17,** 1742–1744
18. Kikuchi, J., Shibayama, N., Yamada, S., Wada, T., Nobuyoshi, M., Izumi, T., Akutsu, M., Kano, Y., Sugiyama, K., Ohki, M., Park, S-Y., Furukawa, Y. (2013) Homopiperazine derivatives as a novel class of proteasome inhibitors with a unique mode of proteasome binding, *PLoS One* **8,** e60649
19. Hideshima, T., Chauhan, D., Richardson, P., Mitsiades, C., Mitsiades, N., Hayashi, T., Munshi, N., Dang, L., Castro, A., Palombella, V., Adams, J., and Anderson, K. C. (2002) NF-κB as a therapeutic target in multiple myeloma. *J. Biol. Chem.* **277,** 16639–16647
20. Hideshima, T., Ikeda, H., Chauhan, D., Okawa, Y., Raje, N., Podar, K., Mitsiades, C., Munshi, N. C., Richardson, P. G., Carrasco, R. D., and Anderson, K. C. (2009) Bortezomib induces canonical nuclear factor-κB activation in multiple myeloma cells. *Blood* **114,** 1046–1052
21. Kikuchi, J., Wada, T., Shimizu, R., Izumi, T., Akutsu, M., Mitsunaga, K., Noborio-Hatano, K., Nobuyoshi, M., Ozawa, K., Kano, Y., and Furukawa, Y. (2010) Histone deacetylases are critical targets of bortezomib-induced cytotoxicity in multiple myeloma. *Blood* **116,** 406–417
22. Drexler, H. G., Matsuo, Y., and MacLeod, R. A. (2003) Persistent use of false myeloma cell lines. *Hum. Cell* **16,** 101–105
23. Shimizu, R., Kikuchi, J., Wada, T., Ozawa, K., Kano, Y., and Furukawa, Y. (2010) HDAC inhibitors augment cytotoxic activity of rituximab by upregulating CD20 expression on lymphoma cells. *Leukemia* **24,** 1760–1768
24. Noborio-Hatano, K., Kikuchi, J., Takatoku, M., Shimizu, R., Wada, T., Ueda, M., Nobuyoshi, M., Oh, I., Sato, K., Suzuki, T., Ozaki, K., Mori, M., Nagai, T., Muroi, K., Kano, Y., Furukawa, Y., and Ozawa, K. (2009) Bortezomib overcomes cell-adhesion-mediated drug resistance through down-regulation of VLA-4 expression in multiple myeloma. *Oncogene.* **28,** 231–242
25. Ri, M., Iida, S., Nakashima, T., Miyazaki, H., Mori, F., Ito, A., Inagaki, A.,

Kusumoto, S., Ishida, T., Komatsu, H., Shiotsu, Y., and Ueda, R. (2010) Bortezomib-resistant myeloma cell lines. A role for mutated *PSMB5* in preventing the accumulation of unfolded proteins and fatal ER stress. *Leukemia* **24,** 1506–1512
26. Kikuchi, J., Shimizu, R., Wada, T., Ando, H., Nakamura, M., Ozawa, K., and Furukawa, Y. (2007) E2F-6 suppresses growth-associated apoptosis of human hematopoietic progenitor cells by counteracting proapoptotic activity of E2F-1. *Stem Cells* **25,** 2439–2447
27. Nonomura, C., Kikuchi, J., Kiyokawa, N., Ozaki, H., Mitsunaga, K., Ando, H., Kanamori, A., Kannagi, R., Fujimoto, J., Muroi, K., Furukawa, Y., and Nakamura M. (2008) CD43, but not P-selectin glycoprotein ligand-1, functions as an E-selectin counter-receptor in human B cell precursor leukemia NALL-1. *Cancer Res.* **68,** 790–799
28. Wada, T., Kikuchi, J., Nishimura, N., Shimizu, R., Kitamura, T., and Furukawa, Y. (2009) Expression levels of histone deacetylases determine the cell fate of hematopoietic progenitors. *J. Biol. Chem.* **284,** 30673–30683
29. Fulciniti, M., Amin, S., Nanjappa, P., Rodig, S., Prabhala, R., Li, C., Minvielle, S., Tai, Y. T., Tassone, P., Avet-Loiseau, H., Hideshima, T., Anderson, K. C., and Munshi, N. C. (2011) Significant biological role of Sp1 transactivation in multiple myeloma. *Clin. Cancer Res.* **17,** 6500–6509
30. Obeng, E. A., Carlson, L. M., Gutman, D. M., Harrington, W. J., Jr., Lee, K. P., and Boise, L. H. (2006) Proteasome inhibitors induce a terminal unfolded protein response in multiple myeloma cells. *Blood* **107,** 4907–4916
31. Mannava, S., Zhuang, D., Nair, J. R., Bansal, R., Wawrzyniak, J. A., Zucker, S.N., Fink, E.E., Moparthy, K. C., Hu, Q., Liu, S., Boise, L. H., Lee, K. P., and Nikiforov, M. A. (2012) KLF9 is a novel transcriptional regulator of bortezomib- and LBH589-induced apoptosis in multiple myeloma cells. *Blood* **119,** 1450–1458
32. Miller, C. P., Rudra, S., Keating, M. J., Wierda, W. G., Palladino, M., and Chandra, J. (2009) Caspase-8 dependent histone acetylation by a novel proteasome inhibitor, NPI-0052. A mechanism for synergy in leukemia cells. *Blood* **113,** 4289–4299
33. Richardson, P., Mitsiades, C., Colson, K., Reilly, E., McBride, L., Chiao, J., Sun, L., Ricker, J., Rizvi, S., Oerth, C., Atkins, B., Fearen, I., Anderson, K., and Siegel, D. (2008) Phase 1 trial of oral vorinostat (suberoylanilide hydroxamic acid, SAHA) in patients with advanced multiple myeloma. *Leuk. Lymphoma.* **49,** 502–507
34. Niesvizky, R., Ely, S., Mark, T., Aggarwal, S., Gabrilove, J. L., Wright, J. J., Chen-Kiang, S., and Sparano, J. A. (2011) Phase 2 trial of the histone deacetylase inhibitor romidepsin for the treatment of refractory multiple myeloma. *Cancer* **117,** 336–342
35. Wada, T., Kikuchi, J., and Furukawa, Y. (2012) Histone deacetylase 1 enhances microRNA processing via deactylation of DGCR8. *EMBO Rep.* **13,** 142–149
36. Bhaskara, S., Knutson, S. K., Jiang, G., Chandrasekharan, M. B., Wilson, A. J., Zheng, S., Yenamandra, A., Locke, K., Yuan, J. L., Bonine-Summers, A. R., Wells, C. E., Kaiser, J. F., Washington, M. K., Zhao, Z., Wagner, F. F., Sun, Z. W., Xia, F., Holson, E. B., Khabele, D., and Hiebert, S. W. (2010) Hdac3 is essential for the maintenance of chromatin structure and genome stability. *Cancer Cell* **18,** 436–447
37. Delcuve, G. P., Khan, D. H., and Davie, J. R. (2013) Targeting class I histone deacetylases in cancer therapy. *Expert. Opin. Ther. Targets* **17,** 29–41
38. Sharma, S. V., Lee, D. Y., Li, B., Quinlan, M. P., Takahashi, F., Maheswaran, S., McDermott, U., Azizian, N., Zou, L., Fischbach, M. A., Wong, K. K., Brandstetter, K., Wittner, B., Ramaswamy, S., Classon, M., and Settleman, J. (2010) A chromatin-mediated reversible drug-tolerant state in cancer cell subpopulations. *Cell* **141,** 69–80
39. Zhang, B., Strauss, A. C., Chu, S., Li, M., Ho, Y., Shiang, K. D., Snyder, D. S., Huettner, C. S., Shultz, L., Holyoake, T., and Bhatia, R. (2010) Effective targeting of quiescent chronic myelogenous leukemia stem cells by histone deacetylase inhibitors in combination with imatinib mesylate. *Cancer Cell* **17,** 427–442
40. Chesi, M., Matthews, G. M., Garbitt, V. M., Palmer, S. E., Shortt, J., Lefebure, M., Stewart, A. K., Johnstone, R. W., and Bergsagel, P. L. (2012) Drug response in a genetically engineered mouse model of multiple myeloma is predictive of clinical efficacy. *Blood* **120,** 376–385
41. Harrison, S. J., Quach, H., Link, E., Seymour, J. F., Ritchie, D. S., Ruell, S., Dean, J., Januszewicz, H., Johnstone, R., Neeson, P., Dickinson, M., Nichols, J., and Prince, H. M. (2011) A high rate of durable responses with romidepsin, bortezomib, and dexamethasone in relapsed or refractory multiple myeloma. *Blood* **118,** 6274–6283
42. Knop, S. (2011) From the observation DAC. Romidepsin revisited. *Blood* **118,** 6231–6232
43. McConkey, D. (2010) Proteasome and HDAC. Who's zooming who? *Blood* **116,** 308–309
44. Chou, T-C. (2010) Drug combination studies and their synergy quantification using the Chou-Talalay method. *Cancer Res.* **70,** 440–446

PLOS | ONE

Homopiperazine Derivatives as a Novel Class of Proteasome Inhibitors with a Unique Mode of Proteasome Binding

Jiro Kikuchi[1], Naoya Shibayama[2], Satoshi Yamada[1], Taeko Wada[1], Masaharu Nobuyoshi[1], Tohru Izumi[3], Miyuki Akutsu[3], Yasuhiko Kano[3], Kanako Sugiyama[4], Mio Ohki[4], Sam-Yong Park[4], Yusuke Furukawa[1]*

1 Division of Stem Cell Regulation, Center for Molecular Medicine, Jichi Medical University, Shimotsuke, Tochigi, Japan, **2** Division of Biophysics, Department of Physiology, Jichi Medical University, Shimotsuke, Tochigi, Japan, **3** Division of Hematology, Tochigi Cancer Center, Utsunomiya, Tochigi, Japan, **4** Protein Design Laboratory, Yokohama City University, Yokohama, Kanagawa, Japan

Abstract

The proteasome is a proteolytic machinery that executes the degradation of polyubiquitinated proteins to maintain cellular homeostasis. Proteasome inhibition is a unique and effective way to kill cancer cells because they are sensitive to proteotoxic stress. Indeed, the proteasome inhibitor bortezomib is now indispensable for the treatment of multiple myeloma and other intractable malignancies, but is associated with patient inconvenience due to intravenous injection and emerging drug resistance. To resolve these problems, we attempted to develop orally bioavailable proteasome inhibitors with distinct mechanisms of action and identified homopiperazine derivatives (HPDs) as promising candidates. Biochemical and crystallographic studies revealed that some HPDs inhibit all three catalytic subunits (ß 1, ß 2 and ß 5) of the proteasome by direct binding, whereas bortezomib and other proteasome inhibitors mainly act on the ß5 subunit. Proteasome-inhibitory HPDs exhibited cytotoxic effects on cell lines from various hematological malignancies including myeloma. Furthermore, K-7174, one of the HPDs, was able to inhibit the growth of bortezomib-resistant myeloma cells carrying a ß5-subunit mutation. Finally, K-7174 had additive effects with bortezomib on proteasome inhibition and apoptosis induction in myeloma cells. Taken together, HPDs could be a new class of proteasome inhibitors, which compensate for the weak points of conventional ones and overcome the resistance to bortezomib.

Citation: Kikuchi J, Shibayama N, Yamada S, Wada T, Nobuyoshi M, et al. (2013) Homopiperazine Derivatives as a Novel Class of Proteasome Inhibitors with a Unique Mode of Proteasome Binding. PLoS ONE 8(4): e60649. doi:10.1371/journal.pone.0060649

Editor: Andrea Cavalli, University of Bologna & Italian Institute of Technology, Italy

Received January 4, 2013; **Accepted** March 1, 2013; **Published** April 11, 2013

Funding: This work was supported in part by the High-Tech Research Center Project for Private Universities: Matching Fund Subsidy from MEXT, a Grant-in-Aid for Scientific Research from JSPS (to Y.F. and J.K.), Adaptable and Seamless Technology transfer Program (A-STEP) from JST, Japan Leukemia Research Fund, Takeda Science Foundation, Kano Foundation, and Mitsui Life Social Welfare Foundation (to J.K.). Y.F. is the winner of the Award in Aki's Memory from the International Myeloma Foundation Japan. The funders had no role in study design, data collection and analysis, decision to publish, or preparation of the manuscript.

Competing Interests: The authors have declared that no competing interests exist.

* E-mail: furuyu@jichi.ac.jp

Introduction

The paradigm of cancer treatment has been dramatically changed by the introduction of small molecular compounds that target the "Achilles' heel" of cancer cells [1]. The proteasome is a proteolytic machinery that executes the degradation of polyubiquitinated proteins to maintain cellular homeostasis [2]. Cancer cells are very sensitive to proteotoxic stress because of intracellular protein overload due to rapid cell cycling and apoptosis inhibition. This feature makes proteasome inhibition a unique and effective way to kill cancer cells that can tolerate conventional therapies [3].

Bortezomib is the first proteasome inhibitor (PI) approved for clinical application, which preferentially targets ß1 and ß5 subunits of the proteasome [3,4]. This drug is particularly effective for multiple myeloma (MM), because it accelerates the unfolded protein response (UPR) via down-regulation of histone deacetylases (HDACs) [5,6] and targets cell adhesion-mediated drug resistance via down-regulation of very late antigen-4 [7,8]. Accordingly, bortezomib is now indispensable for the treatment of MM in combination with other anti-cancer drugs including alkylating agents, corticosteroids and HDAC inhibitors [9–11].

Although bortezomib therapy is a major advance in clinical oncology, there are at least three major problems to be resolved as soon as possible. First, bortezomib has several possible off-target toxicities [12,13]. Second, the development of intrinsic and acquired resistance to bortezomib is an emerging problem [14–19]. Third, bortezomib should be administered intravenously on biweekly schedules with treatment periods extending for 6 months or more. The development of orally bioavailable PIs with distinct mode of action is a possible way to circumvent these issues.

Homopiperazine-derived compounds have been developed as orally active agents because of their superb bioavailability. Among them, dilazep, an inhibitor of nucleoside transporters, has been clinically used for the treatment of cardiac dysfunction via post-oral administration [20]. Some homopiperazine derivatives (HPDs), such as K-7174 and K-11706, were shown in pre-clinical studies to inhibit cell adhesion [21] and to rescue anemia of chronic disorders via the activation of erythropoietin production *in vitro* and *in vivo* [22,23]. In addition, K-7174 was reported to

exert anti-inflammatory action via induction of the UPR [24]. These observations prompted us to consider that HPDs could be orally active PIs; however, this possibility has not been tested so far. In this study, we demonstrated that HPDs, including K-7174, have the ability to inhibit proteasome activity via different mechanisms of action from bortezomib and other conventional PIs.

Materials and Methods

Cells and Cell Culture

We used cell lines from acute lymphoblastic leukemia (KOPM30 and Jurkat), mantle cell lymphoma (HBL-2, Granta519 and NCEB-1), Burkitt lymphoma (Daudi and Namalwa), multiple myeloma (KMS12-BM, RPMI8226, U266, KMM1 and Delta47) [25], acute myeloid leukemia (HL60, KG1a and U937) and chronic myeloid leukemia (K562) in this study. These cell lines were purchased from the Health Science Research Resources Bank (Osaka, Japan) except for KOPM30, which was provided by Dr. Takeshi Inukai (University of Yamanashi, Yamanashi, Japan) [26], and Granta519 and NCEB-1, which were provided by Professor Martin J. S. Dyer (Leicester University, Leicester, UK) [27], and maintained in RPMI1640 medium (Sigma Co., St. Louis, MO) supplemented with 10% heat-inactivated fetal calf serum (Sigma) and antibiotics.

Drugs

HPDs and bortezomib were provided by Kowa (Tokyo, Japan) and Millennium Pharmaceuticals (Cambridge, MA), respectively. The compounds were dissolved in dimethyl sulfoxide (DMSO), diluted with 0.9% NaCl at appropriate concentrations and stored at −80°C until use. The chemical structures of K-7174 (N,N'-bis-(E)-(5-(3,4,5-trimethoxy-phenyl)-4-pentenyl) homopiperazine) and other HPDs are shown in Table 1.

Cell Proliferation Assay

Cell proliferation was measured by the 3-(4,5-dimethylthiazol-2-yl)-2,5-diphenyltetrazolium (MTT) reduction assay using a Cell Counting Kit (Wako Biochemicals, Osaka, Japan). Absorbance at 450 nm was analyzed with a microplate reader and expressed as a percentage of the value of corresponding untreated cells.

Immunoblotting

Immunoblotting was carried out according to the standard method using the following antibodies: anti-ubiquitin, anti-ubiquityl histone H2A (Lys119), anti-K48-linked polyubiquitin (Cell Signaling Technology, Beverly, MA), anti-proteasome ß5 subunit (PSMB5) (Enzo Life Sciences, Farmingdale, NY), and anti-GAPDH (Santa Cruz Biotechnology, Santa Cruz, CA) [28].

20 S Proteasome Activity Assay

Proteasome activity assays were performed using 20 S proteasome assay kits (Enzo Life Sciences and Cayman Chemical, Ann Arbor, MI). Proteasomal chymotrypsin-like, trypsin-like and caspase-like activities were determined using fluorogenic substrates suc-LLVY-amc, boc-LRR-amc, and z-LLE-amc (Enzo Life Sciences), respectively, with purified human erythrocyte-derived 20 S proteasome (Enzo Life Sciences) or MM cell lysates. Reactions were initiated by enzyme or lysate addition, and monitored for amc product formation at 30°C on a spectrofluorometer (SpectraMax Gemini EM; Molecular Devices, Sunnyvale, CA) using excitation of 360 nm and emission of 480 nm [29,30].

X-ray Crystallographic Analysis of the K-7174/proteasome Complex

Single crystals of 20 S proteasome from *Saccharomyces cerevisiae* (Enzo Life Sciences) in complex with K-7174 were grown using the sitting drop vapor diffusion method at 20°C by mixing 8 µl of protein and 8 µl of reservoir solution. The protein concentration used for crystallization was 10 mg/ml in 10 mM Tris-HCl (pH 7.5) and 1 mM EDTA. The reservoir solution contained 4.5% (v/v) 2-methyl-2,4-pentanediol (MPD), 36 mM magnesium acetate, 90 mM morpholino-ethane-sulphonic acid (MES, pH 7.2), 10% (v/v) DMSO, and 12.5 mM K-7174. Crystals were soaked in cryoprotectant buffer containing 30% (v/v) MPD and flash frozen in liquid nitrogen. X-ray data were collected at beamline BL44XU of Spring-8 (Hyogo, Japan) equipped with an MAR CCD detector 225 mm at 100 K under a nitrogen gas stream. The wavelength of the incident X-ray was 1.0 Å. Diffraction data sets were processed with HKL2000, and scaled with SCALEPACK [31]. The crystals belonged to the space group $P2_1$ with unit cell parameters of $a=134.26$, $b=301.36$, $c=143.96$ and $\beta=112.9°$. The structures were solved by molecular replacement using MOLREP [32] with the previously reported structure of 20 S proteasome (Protein Data Bank code 1RYP) as a starting model. The best solution using data from 40 to 3.5 Å resolution range yielded a correlation coefficient of 0.7 and an *R*-factor of 0.33 for structure, after rigid body refinement. At this stage, crystallo-

Table 1. Chemical structures of homopiperazine derivatives used in this study.

Compound	Chemical formula	Number of carbon atom chains
K-7174	N,N'-bis-(E)-[5-(3,4,5-trimethoxy-phenyl)-4-pentenyl] homopiperazine	C=5
K-7259	N,N'-bis-[4-(3,4,5-trimethoxy-phenyl)-butyl] homopiperazine	C=4
K-7220	N,N'-bis-[3-(3,4,5-trimethoxy-phenyl)-propyl] homopiperazine	C=3
K-10310	N,N'-bis-(E)-[6-(3,4,5-trimethoxy-phenyl)-4- oxo-5-hexenyl] homopiperazine	C=6
K-10252	N,N'-bis-(E)-[7-(3,4,5-trimethy-phenyl)-5-oxo-6- heptenyl] homopiperazine	C=7
K-10228	N,N'-bis-(E)-[5-(3,4,5-trimethyl-phenyl)-4- pentenyl] homopiperazine	C=5
K-10256	N,N'-bis-(E)-[5-(2,3,4,5-tetramethoxy-phenyl)-4- pentenyl] homopiperazine	C=5
K-10487	N,N'-bis-(E)-[4-(3,4,5-trimethoxy-naphthyl)-butyl] homopiperazine	C=5
K-10552	N,N'-bis-(E)-[5-(3,4,5-trimethoxy-phenyl)-4- pentenyl]-6-methoxy-homopiperazine	C=5

doi:10.1371/journal.pone.0060649.t001

graphic refinement was pursued in PHENIX [33]. After an initial round of simulated annealing refinement, several macrocycles that included bulk solvent correction, anisotropic scaling of the data, individual coordinate refinement with minimization, and individual isotropic ADP (atomic displacement parameters) refinement were carried out with maximum likelihood as a target. In the course of the refinement, K-7174 compound and water molecules were added to the models by manual inspection of their positions in both 2*Fo*-*Fc* and *Fo*-c maps, and individual ADP refinement was carried out in the final stages. Map fitting and other manipulations with molecular models were performed using the graphic software COOT [34]. The stereochemistry of the final models was assessed using MolProbity [35]. Data collection and refinement statistics are summarized in Table 2. Atomic coordinates and structure factors of the complex have been deposited in the Protein Data Bank under accession code 4EU2.

Establishment of Bortezomib-resistant MM Cell Lines

To confer bortezomib resistance to MM cells, we transduced with mutated *PSMB5* cDNA as described previously [17]. A mutation was inserted at nucleotide position 322 (G/A) by PCR-based site directed mutagenesis using wild-type *PSMB5* cDNA (obtained from OpenBiosystems, Thermo Fisher Scientific, Huntsville, AL) as a template. Mutated *PSMB5* cDNA was inserted into a lentiviral vector CSII-CMV-MCS-IRES-VENUS (kindly provided by Dr. Hiroyuki Miyoshi, RIKEN BioResorce Center, Ibaraki, Japan) [36]. Wild-type *PSMB5* cDNA was also inserted into the same vector and used as a control. These vectors were co-transfected into 293FT cells with packaging plasmids (Invitrogen, Carlsbad, CA) to produce infective lentiviruses in culture supernatants as previously described [37]. RPMI8226 cells were infected with each viral supernatant for 24 h. We collected VENUS-positive cells using a FACSaria flow cytometer (Becton Dickinson, Bedford, MA) and seeded them at one cell/well in a 96-well plate to obtain single cell clones.

Isobologram Analysis of Drug Interaction

The cytotoxic interaction of bortezomib and K-7174 was evaluated at the point of IC_{80} by the isobologram of Steel and Peckham. The IC_{80} was defined as the concentration of drugs that produced 80% inhibition of cell growth. The theoretical basis of the isobologram method has been described in detail previously [38]. Briefly, the envelope of additivity is constructed from dose–response curves of the combined drugs. The combination is regarded as additive when the data points of the drug combination fall within the envelope of additivity. The drug combination is regarded as supra-additive (synergism) and antagonistic when the data points fall to the left and the right of the envelope, respectively.

Results

Homopiperazine Derivatives Inhibit Proteasome Activities

The ability of K-7174 to elicit the UPR prompted us to speculate that this drug could inhibit proteasome activity [5,6,24]. To test this idea, we incubated purified human erythrocyte-derived 20 S proteasome with K-7174 and eight HPDs, which are structurally similar to K-7174 (Table 1), and measured chymotrypsin-like (ß5), caspase-like (ß1), and trypsin-like (ß2) activities of the proteasome using specific fluorogenic peptides. As shown in Fig. 1A, six out of nine HPDs significantly inhibited proteasome activities of the purified 20 S proteasome. We performed the same experiments with cell-based assays using RPMI8226 cells to confirm the proteasome-inhibitory effect of the six HPDs (Fig. 1B). Interestingly, HPDs inhibited all three catalytic subunits with similar kinetics, suggesting a different mechanism of action from bortezomib.

Among the HPDs examined, K-7174, K-10256, K-10487 and K-10552 showed relatively strong effects on proteasome activities. They commonly possess methoxy-phenyl groups and pentenyl arms (with five carbon atom chains; C = 5) (Table 1). In contrast, proteasome-inhibitory activity was weak or none in K-7259 and

Table 2. Statistics of crystallographic analysis.

Space group/unit cell(Å)	***P*21/*a*=134.26, *b*=301.36, *c*=143.96, ß=112.9°**
Resolution range (Å)	50.0–2.5
Reflections (Measured/Unique)	313,772/962,020
Completeness (Overall/Outer Shell, %) [a]	88.5/72.3
R-merge (Overall/Outer Shell, %)[a, b]	10.1/28.0
Redundancy (Overall)	3.1
Mean <Ió/(I)> (Overall)	12.2
Overall *B*-factor from Wilson plot (Å^2)	22
Refinement statistics	
R-work[c]/*R-free* (%)[c]	20.2/25.5
R.m.s.d. bond lengths/bond angles (Å)	0.008/1.178
Average *B*-factor (protein/water/compound, Å^2)	39/31/82
Ramachandran plot	
Favored/allowed/outlier (%)	95.86/3.82/0.32

[a]Completeness and *R*-merge, are given for overall data and for the highest resolution shell.
The highest resolution shells for the dataset were 2.54–2.50 Å.
[b]*R*merge = $\sum$ | I_i – <*I*> |/$\sum|I_i|$; where I_i is intensity of an observation and <*I*> is the mean value of that reflection and the summations are over all equivalents.
[c]*R-work* = $\sum_h$ || *Fo(h)* | – | *Fc(h)* ||/$\sum_h$*Fo(h)*; where *Fo* and *Fc* are the observed and calculated structure factor amplitudes, respectively. The *R-free* was calculated with 5% of the data excluded from the refinement.
doi:10.1371/journal.pone.0060649.t002

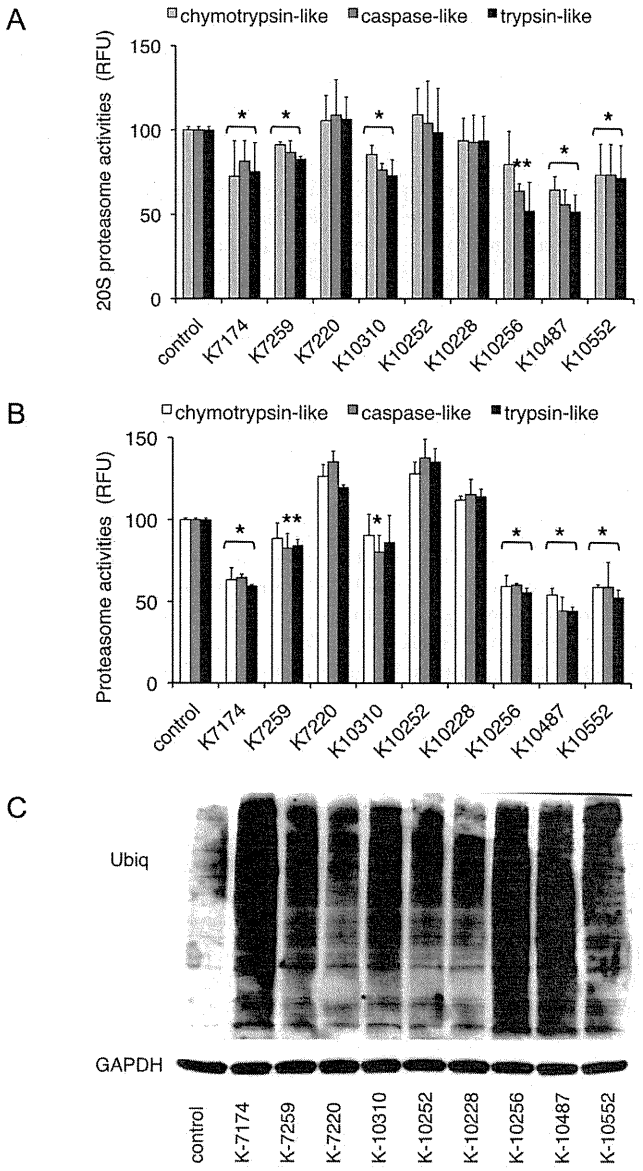

Figure 1. Inhibition of 20 S proteasome activity by homopiperazine derivatives. A. Purified erythrocyte-derived 20 S proteasome was incubated in the absence (control) or presence of the indicated HPDS at 5 μM. Chymotrypsin-like, caspase-like and trypsin-like activities were determined by measuring fluorescence generated from the cleavage of specific substrates. Results are represented as relative fluorescence units (RFU) with control set at 100%. The means ± S.D. (bars) of three independent experiments are shown. *P*-values were calculated by one-way ANOVA with the Student-Newman-Keuls multiple comparisons test. Asterisks indicate $p<0.05$ against corresponding controls. B. RPMI8226 cells were treated with or without 5 μM HPDs, and analyzed for proteolytic activities as described above. C. RPMI8226 cells were cultured in the absence (control) or presence of 10 μM HPDs for 24 hours, and subjected to immunoblotting for ubiquitinated proteins and GAPDH (internal control).
doi:10.1371/journal.pone.0060649.g001

K-7220, which have shorter arms (C = 4 and 3, respectively), and K-10310 and K-10252, which have longer arms (C = 6 and 7, respectively), although all of them possess trimethoxy-phenyl groups (Table 1). The inhibitory effect was also undetected in K-10228, which has trimethyl-phenyl groups instead of trimethoxy-phenyl groups and pentenyl arms (C = 5) (Fig. 1A and B). Consistent with these data, immunoblot analysis revealed a marked accumulation of ubiquitinated proteins in RPMI8226 cells treated with K-7174, K-10256, K-10487 and K-10552 but not K-7259, K-7220, K-10252 and K-10228 (Fig. 1C). These results suggest that the trimethoxy-phenyl group at the tip of the pentenyl arm (C = 5) is a critical structure of homopiperazine-derived proteasome inhibitors. Based on this finding, K-7174 was selected as the most promising candidate for pharmaceutical development as a PI and was further characterized in this study.

K-7174 Inhibits Proteasome Activities in a Distinct Manner from Bortezomib

First, we compared the proteasome-inhibitory activity of K-7174 with that of bortezomib. As shown in Fig. 2A, K-7174 similarly inhibited all three subunits in a dose-dependent fashion, whereas bortezomib did not affect trypsin-like activity but efficiently inhibited chymotrypsin- and caspase-like activities. This pattern was readily reproducible in cell-based assays using RPMI8226 (Fig. 2B) and other myeloma cell lines (data not shown).

Next, we monitored the accumulation of ubiquitinated proteins in K-7174-treated MM cells in comparison with bortezomib. As shown in Fig. 2C and D, K-7174 induced a marked accumulation of ubiquitinated proteins in all three cell lines in a dose- and time-dependent fashion, as did bortezomib. In addition, we detected the accumulation of lysine 48-linked polyubiquitinated proteins and ubiquityl histone H2A, both of which represent specific and critical modifications leading to proteasomal degradation, in both K-7174- and bortezomib-treated MM cells (Fig. 2E). These results indicate that K-7174 is a novel PI distinct from bortezomib in its chemical structure and effects on proteasome activity.

K-7174 Interacts with the Catalytic Domains of ß1, ß2 and ß5 Subunits of the Proteasome in a Distinct Manner from Bortezomib

To understand the mechanisms of proteasome inhibition by K-7174, we determined the X-ray crystal structure of the yeast 20 S proteasome in complex with K-7174 at 2.5 Å resolution (Table 2). Analysis of the structure revealed that three molecules of K-7174 bind to and block the active sites of all three catalytic ß-type subunits, ß1, ß2 and ß5, with a similar binding mode (Fig. 3A), consistent with the biochemical data. Figure 3B shows the conformation and binding mode of K-7174 near the ß5 active site for example. The electron density of K-7174 was well-defined except for one trimethoxy-phenyl group near the ß4 subunit, which was partially discorded (Fig. 3B). The overall binding is determined largely by hydrophobic interactions between K-7174 and Gly47, Met97, Asp118, Gly130 and Ser131 of the ß5 subunit as well as Arg22 and Gly23 of the ß4 subunit (Fig. 3B). Importantly, the oxygen atom of the methoxy group of K-7174 makes a hydrogen bond (with a distance of 2.9 Å) to the OH group of the N-terminal threonine residue (Thr1), which acts as a nucleophile in hydrolysis. We also observed that, despite some difference in binding interactions, the active sites of the ß1 and ß2 subunits are blocked by the trimethoxy-phenyl group of K-7174 in a similar fashion to that observed in the ß5 subunit (Fig. 3C). These findings are fully compatible with our conclusion from biochemical analyses, and confirmed that the trimethoxy-phenyl group, but not the trimethyl-phenyl group, interacts with the active sites of three catalytic subunits via hydrogen bonding and the pentenyl arm (C - 5) fits the hydrophobic grooves between ß subunits via hydrophobic interaction. It is highly likely that K-10256, K-10487 and K-10552 interact with ß-subunits in a similar

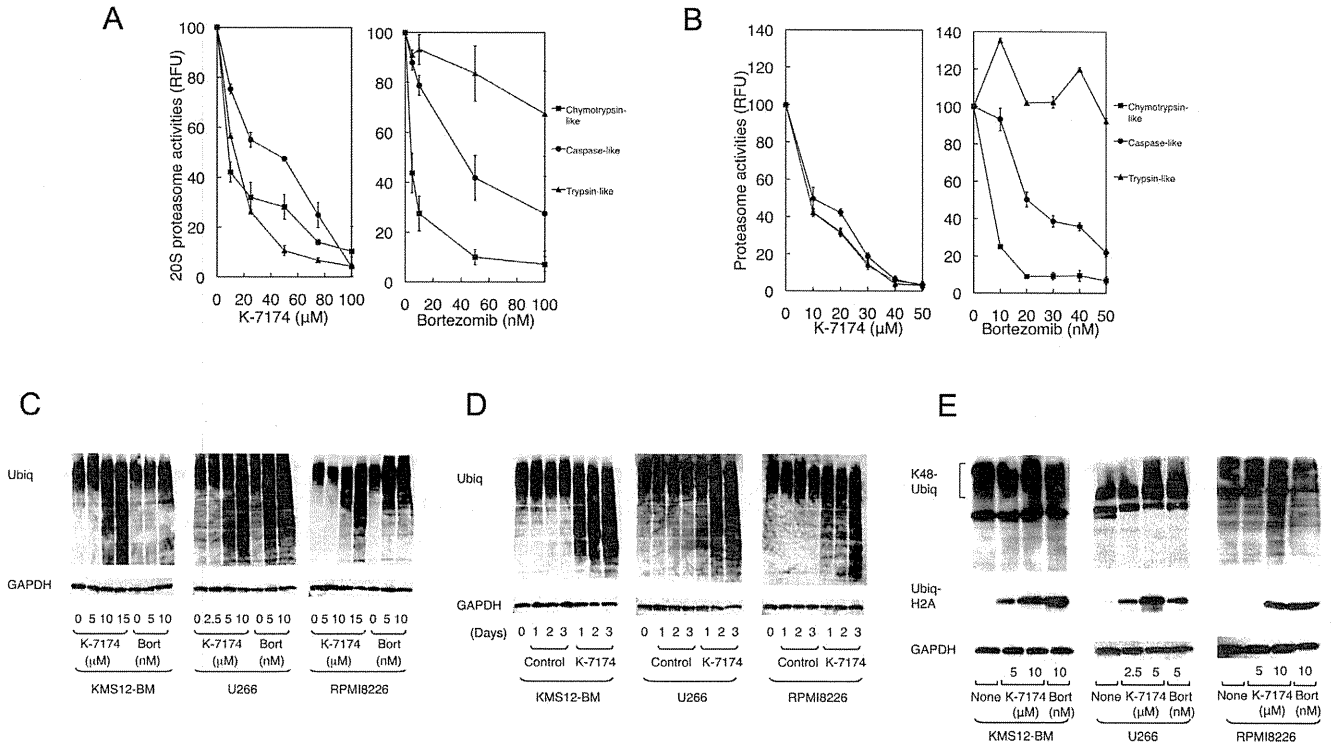

Figure 2. Inhibition of 20S proteasome activity by K-7174. A. We treated purified erythrocyte-derived 20 S proteasome with either K-7174 or bortezomib at the indicated doses and determined chymotrypsin-like, caspase-like and trypsin-like activities as described in the legend of Fig. 1. B. RPMI8226 cells were treated with either K-7174 or bortezomib at the indicated doses, and analyzed for proteolytic activities. C. MM cell lines (KMS12-BM, U266, and RPMI8226) were cultured with K-7174 or bortezomib (Bort) at the indicated doses for 48 hours. Whole cell lysates were subjected to immunoblotting for ubiquitinated proteins and GAPDH (internal control). D. MM cell lines were cultured with either K-7174 (5 μM for U266 and 10 μM for KMS12-BM and RPMI8226) or the vehicle alone (Control) for up to 3 days. Whole cell lysates were prepared at given time points and subjected to immunoblotting as described above. E. MM cell lines were cultured in the absence (None) or presence of K-7174 or bortezomib (Bort) at the indicated doses for 48 hours, and subjected to immunoblotting for lysine48-linked polyubiquitinated proteins (K48-Ubiq), ubiquityl histone H2A (Ubiq-H2A), and GAPDH (internal control).
doi:10.1371/journal.pone.0060649.g002

manner. Taken together, these results provide the molecular basis of HPDs' ability to inhibit all three catalytic subunits at the same time.

Cytotoxic Effects of Homopiperazine Derivatives on Hematological Malignancies *in vitro*

Given the proteasome-inhibitory action of HPDs, we investigated whether these agents exert cytotoxic activity against myeloma and other hematological malignancies. To this end, we cultured various cell lines with K-7174 and K-10487, and determined IC_{50} values using MTT assays. As shown in Fig. 4A, both agents showed remarkable cytotoxicity at ~10 μM in most cell lines. The cytotoxic doses were virtually identical to the proteasome-inhibitory concentrations, suggesting that K-7174 and K-10487 exert cytotoxic effects mainly via proteasome inhibition. Consistent with this notion, the cytotoxic activity of both K-7174 and bortezomib was mediated via the caspase-8-dependent pathway (manuscript in preparation). However, the sensitivity pattern was obviously different between HPDs and bortezomib, implying a difference in their mechanisms of action.

Comparison of the Binding Modes of K-7174 and Bortezomib

To gain mechanistic insights, we compared the binding mode of K-7174 with that of bortezomib using X-ray crystallographic data. As shown in Fig. 4B, three molecules of K-7174 bind to the active pockets of the ß1, ß2 and ß5 subunits along hydrophobic grooves in the direction of the ß7, ß1 and ß4 subunits, respectively. In contrast, bortezomib is attached to the ß5 subunit by a hydrogen-bond network composed of Ala49, Thr21 and Gly44 [39] (Fig. 4B and C). Mutations of amino acids within or near the bortezomib-binding pocket in the ß5 subunit, such as Ala49, Thr21, Met45 and Cys52, were reported to cause bortezomib resistance by reducing the affinity to the drug (14–19). Among them, Ala49 makes a direct hydrogen bond to bortezomib, explaining why this position is most frequently mutated in bortezomib-resistant cells. Furthermore, a Cys52Phe or Met45Val substitution results in a steric clash between the side chains of these two residues (Fig. 4C), leading to repulsion of bortezomib from the binding pocket [14,16,17]. In contrast, these mutations should not affect the affinity of K-7174 to ß5 subunit, because the binding site of K-7174 is spatially distinct from the bortezomib-binding pocket (Fig. 4B and C).

K-7174 Overcomes Bortezomib Resistance caused by a ß5-subunit Mutation

Because K-7174 appears to inhibit proteasome activity with a distinct mode from bortezomib, it is anticipated that K-7174 is effective for bortezomib-resistant cells. Previous studies revealed that a mutation of the *PSMB5* gene at nucleotide position 322 (G322A), which corresponds to the substitution of Ala49 to Thr (Ala49Thr), induced conformational changes in the bortezomib-

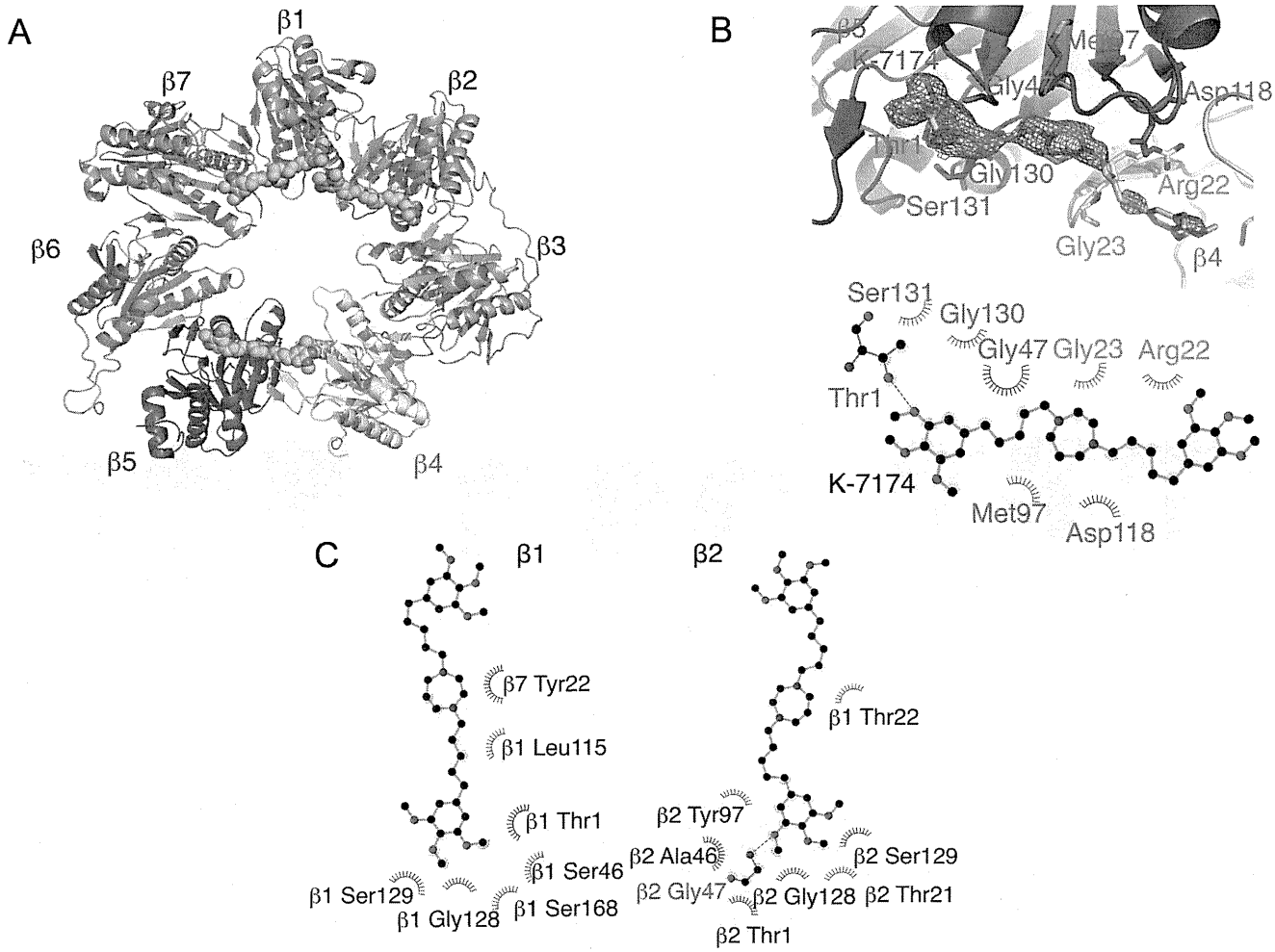

Figure 3. Crystallographic structure of the K-7174/proteasome complex. A. An overall ribbon diagram showing the folds of ß1 to ß7 subunits in the proteasome. The ß4 and ß5 subunits are colored yellow and blue, respectively. The K-7174 molecules bound to each ß subunit are shown as a space-filling representation colored green. Red spots indicate oxygen atoms. B. The final averaged electron density map (2*Fo-Fc*) covering K-7174 is shown (contoured at 1∂) (upper panel). A schematic diagram showing the interactions between K-7174 and the ß4 and ß5 subunits. The residues of ß4 and ß5 subunits associated with K-7174 are colored yellow and blue, respectively. A hydrogen bond is shown as a green dotted line (lower panel). C. A schematic diagram showing the interactions between K-7174 and the ß1 and ß2 subunits. The residues of ß1 and ß2 subunits associated with K-7174 are shown. A hydrogen bond is shown as a green dotted line.
doi:10.1371/journal.pone.0060649.g003

binding pocket of ß5 subunit and was responsible for acquired bortezomib resistance in T-cell acute lymphoblastic leukemia and myeloid leukemia cells [14–16]. Recently, Ri *et al.* [17] reported the establishment of bortezomib-resistant MM cell lines by transduction with G322A-mutated *PSMB5* cDNA. Taking the same approach, we established three mutant sublines (mutant-5B, 5F and 9B) from RPMI8226 cells lentivirally transduced with mutated *PSMB5* along with a marker gene *VENUS*. As controls, three wild-type sublines (WT-4G, 8F and 9G) were concomitantly established by mock transfection. We selected mutant-5F and WT-9G as representative sublines after determining the sensitivity to bortezomib (data not shown). The expression levels of VENUS and PSMB5 were virtually identical in these sublines (Fig. 5, A and B). As expected, sensitivity to bortezomib was significantly lower in the mutant subline than in the WT subline in MTT assays (Fig. 5C). In striking contrast, K-7174 induced cytotoxicity equally in WT and mutant sublines (Fig. 5C). In correlation with the results of MTT assays, K-7174 inhibited chymotrypsin-like (ß5) activity similarly in both sublines, whereas bortezomib could only partially inhibit the activity in the mutant subline (data not shown). These results were fully reproducible in other WT and mutant sublines (data not shown). To confirm the effects on proteasome activities, we determined the accumulation of ubiquitinated proteins in these sublines. As shown in Fig. 5D, ubiquitinated proteins were accumulated to a lesser extent in mutant cells than WT cells when they were treated with bortezomib (right panel). In contrast, K-7174 similarly induced intracellular protein ubiquitination in WT and mutant sublines (Fig. 5D, left panel). These results suggest that K-7174 can overcome bortezomib resistance.

K-7174 and Bortezomib Exert Additive Cytotoxicity Against MM Cells

As K-7174 inhibits proteasome activity in a distinct manner from bortezomib, their combination would be additive and useful for dose reduction of bortezomib. Indeed, K-7174 additively enhanced the proteasomal ß5-inhibitory effect of bortezomib (Fig. 6A) as well as bortezomib-induced accumulation of ubiquitinated proteins (Fig. 6B). Furthermore, isobologram anal-

A

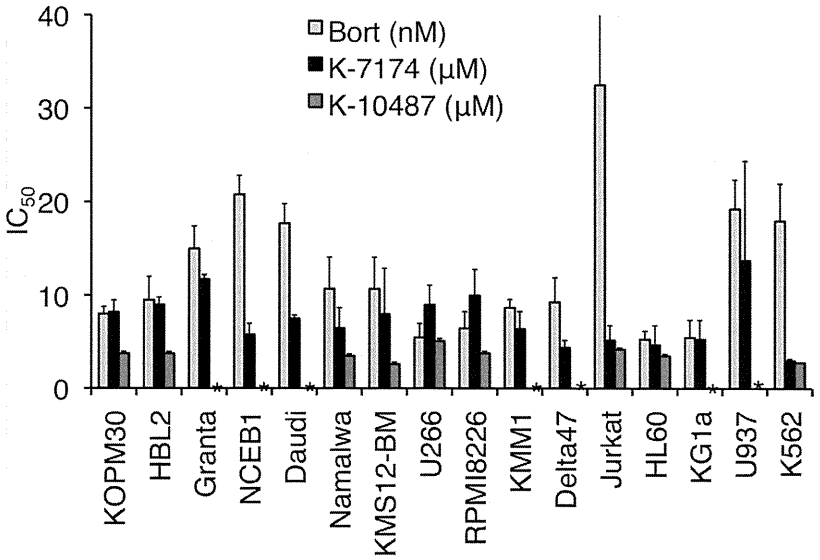
40
30
20
10
0
IC50
Bort (nM)
K-7174 (μM)
K-10487 (μM)
KOPM30
HBL2
Granta
NCEB1
Daudi
Namalwa
KMS12-BM
U266
RPMI8226
KMM1
Delta47
Jurkat
HL60
KG1a
U937
K562

B

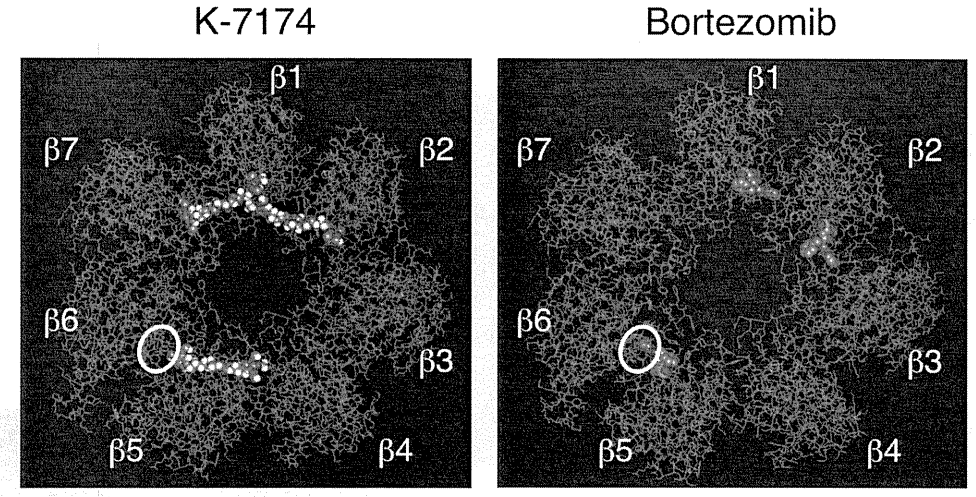
K-7174
Bortezomib
β1
β2
β3
β4
β5
β6
β7

C

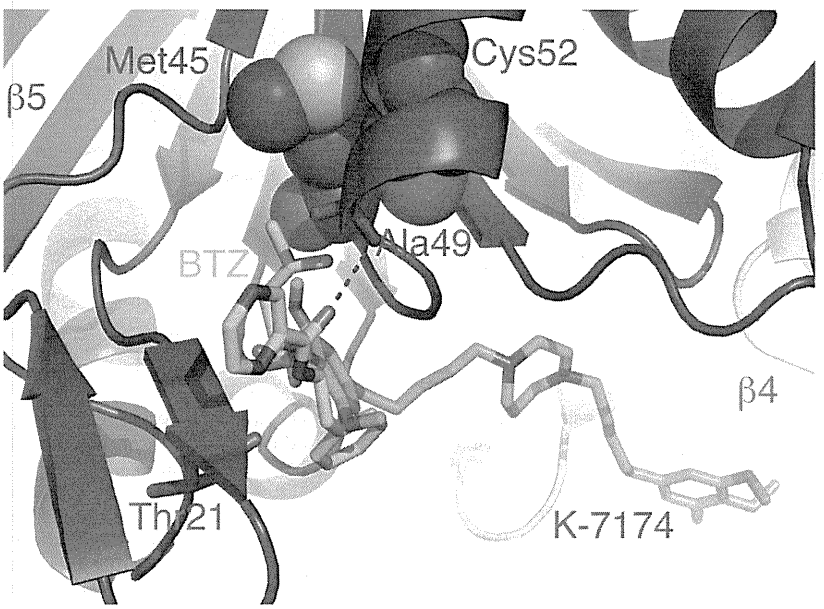
Met45
Cys52
β5
Ala49
BTZ
β4
Thr21
K-7174

Figure 4. Comparison of K-7174 and bortezomib in cytotoxic activity and proteasome binding. A. Cell proliferation was measured by MTT assays after culturing with serially diluted K-7174, K-10487 and bortezomib for 72 hours. Absorbance at 450 nm was analyzed with a microplate reader, and expressed as a percentage of the value of corresponding untreated cells. The IC_{50} value was defined as the concentration of each drug that produces 50% inhibition of cell growth. The means ± S.D. (bars) of three independent experiments are shown. Asterisks indicate "not determined". B. Overall crystallographic structures showing the folds of ß1 to ß7 subunits in the proteasome bound with K-7174 (left panel) and bortezomib (right panel). Mutation sites observed in bortezomib-resistant cells are circled. C. Structure of the proteasome in complex with bortezomib (PDB cord 2F16) overlapped that with K-7174 described here. Only the protein atoms of the bortezomib-bound form are shown. Bortezomib-resistant mutant residues (Ala49, Thr21, Cys52 and Met45) are colored red and shown as a space-filling diagram.
doi:10.1371/journal.pone.0060649.g004

ysis of drug interaction revealed that K-7174 and bortezomib showed additive cytotoxicity in MM cell lines (Fig. 6C).

Discussion

In the present study, we show that HPDs constitute a novel class of PIs with a unique mode of proteasome binding. Although many kinds of small molecular PIs with various chemical structures have been developed [40,41], this is the first demonstration of the proteasome-inhibitory activity of HPDs. In addition, most of the previous PIs mainly acted on one or two catalytic subunits and their mechanisms of action are not fully understood [40,41]. In contrast, we have demonstrated that HPDs act on all three catalytic subunits of the proteasome by direct binding to the active pockets of the ß1, ß2 and ß5 subunits with a similar binding mode and kinetics. These results indicate the unique features of homopiperazine-derived PIs in chemical structures and effects on the proteasome. Moreover, we have identified the critical chemical structure of homopiperazine-derived PIs; therefore, these observations may contribute to the development of novel PIs with higher activity and specificity.

The high concentrations to trigger cytotoxicity might be the obstacle for clinical application of K-7174. Crystal structure analyses revealed that K-7174 interacts with ß subunits largely via

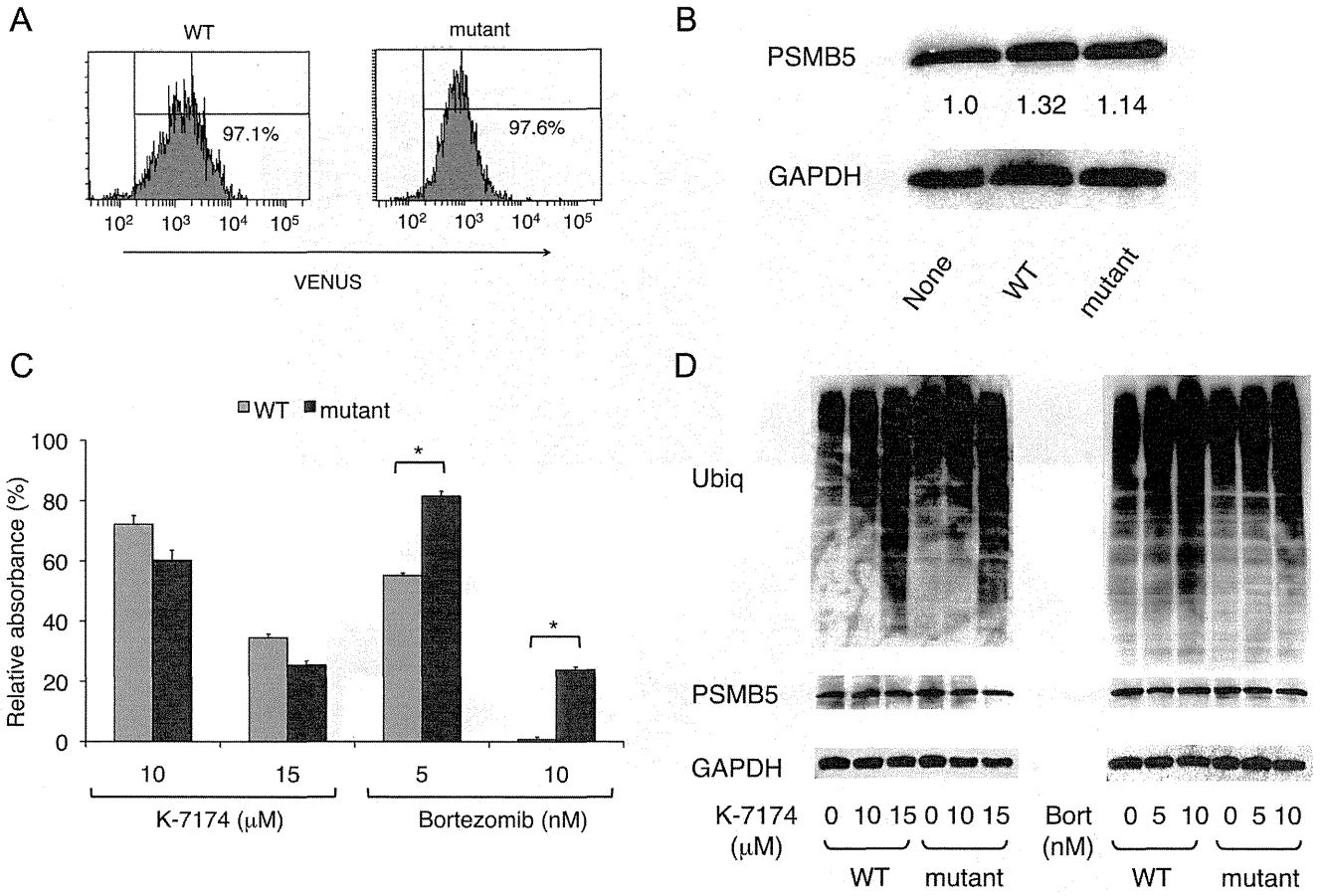

Figure 5. Cytotoxic effects of K-7174 on bortezomib-resistant MM cells. We established wild-type (WT) and mutant (mutant) sublines from RPMI8226 by transducing with wild-type and mutated *PSMB5* cDNA, respectively, and analyzed the expression of VENUS by flow cytometry (A) and proteasome ß5 subunit by immunoblotting (B). The signal intensities of ß5 subunit (PSMB5) were quantified, normalized to those of the corresponding GAPDH, and shown as relative values in the panel B. C. Cell proliferation was measured by MTT assays after culturing each subline with either K-7174 or bortezomib at the indicated doses for 72 hours. Results are represented as relative absorbance with untreated control set at 100%. The means ± S.D. (bars) of three independent experiments are shown. *P*-values were calculated by one-way ANOVA with the Student-Newman-Keuls multiple comparisons test. Asterisks indicate $p<0.01$ against the WT subline. D. Each subline was cultured with either K-7174 or bortezomib (Bort) at the indicated doses for 48 hours. Whole cell lysates were subjected to immunoblotting for cellular protein ubiquitination, proteasome ß5 subunit (PSMB5) and GAPDH (internal control).
doi:10.1371/journal.pone.0060649.g005

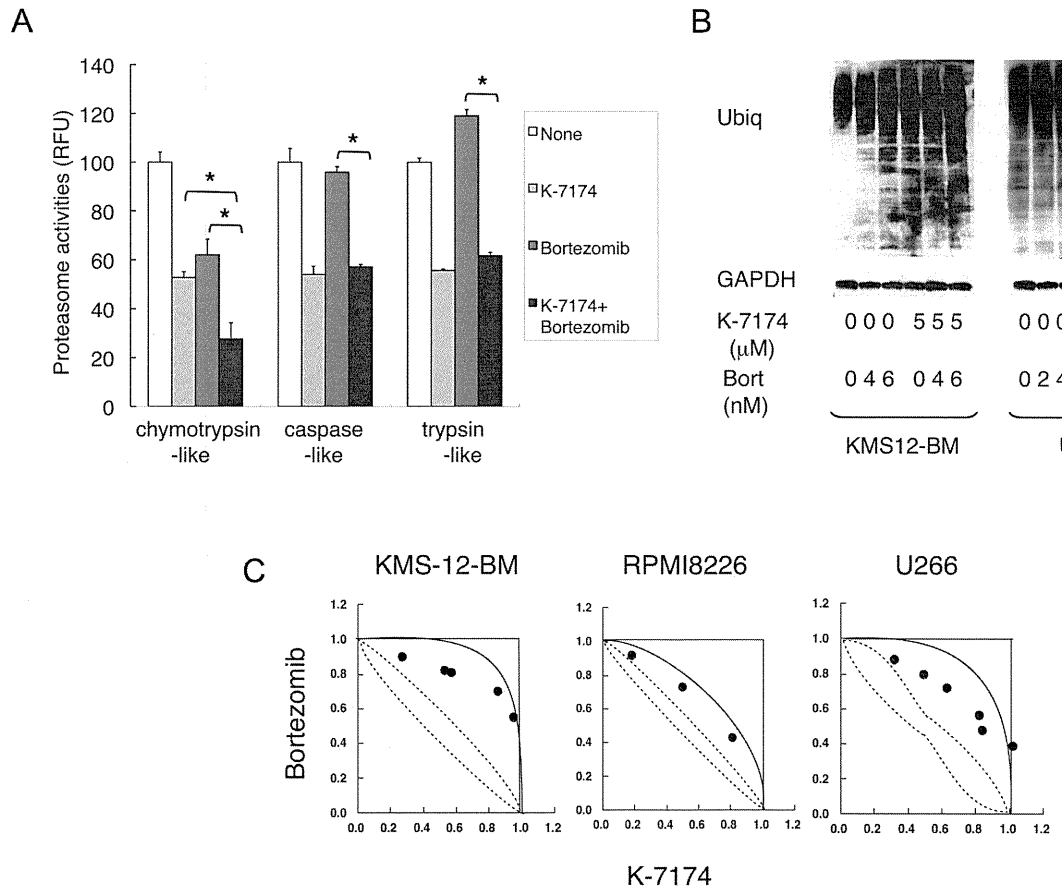

Figure 6. K-7174 and bortezomib exert additive cytotoxicity against MM cell. A. We treated RPMI8226 cells with K-7174 (10 μM), bortezomib (5 nM) or both agents, and determined chymotrypsin-like, caspase-like and trypsin-like activities. Results are represented as relative fluorescence units (RFU) with vehicle controls set at 100%. The means ± S.D. (bars) of three independent experiments are shown. Asterisks indicate $p<0.01$ by paired Student's *t*-test. B. We cultured KMS12-BM, U266 and RPMI8226 cells in the absence or presence of K-7174, bortezomib or both agents for 48 hours at the indicated doses. Whole cell lysates were subjected to immunoblotting for ubiquitinated proteins and GAPDH (internal control). Data are representative of multiple independent experiments. C. Isobolograms of simultaneous exposure of three MM cell lines to K-7174 and bortezomib. The concentrations that produced 80% growth inhibition are expressed as 1.0 on the ordinate and abscissa of isobolograms. The envelope of additivity, surrounded by solid and broken lines, was constructed from dose–response curves of bortezomib and K-7174. The combination is regarded as additive, because all data points fall within the envelope of additivity. The isobolograms shown are representative of at least three independent experiments. Each point represents the mean of at least three independent experiments; standard deviations were less than 25% and were omitted.
doi:10.1371/journal.pone.0060649.g006

hydrophobic interaction, whereas bortezomib binds to the ß5 subunit via a hydrogen-bond network, explaining why higher concentrations are required for HPDs compared with bortezomib. Therefore, the development of novel HPDs with higher activity and specificity is essential for clinical translation. Our finding on the chemical structure of homopiperazine-derived PIs may be of great help in this regard.

Despite the great success of bortezomib in the treatment of refractory malignancies such as MM and mantle cell lymphoma [3,4], we still intend to develop orally bioavailable PIs with distinct mechanisms of action from bortezomib. Several novel PIs, such as carfilzomib [42,43], NPI-0052 [44], CEP-18770 [45], MLN9708 [46], and ONX-0912 [47], are now undergoing clinical trials and show considerable benefits for refractory/relapsed cases as well as untreated MM patients. Among them, carfilzomib and its derivative ONX-0912 are peptide derivatives and have greater selectivity for the ß5 subunit than bortezomib. Although NPI-0052 is a non-peptide PI targeting all three proteasome subunits, its effect was strong for chymotrypsin-like (ß5), moderate for trypsin-like (ß2), and weak for caspase-like (ß1) activities [44]. In addition, NPI-0052 is intravenously administered in clinical studies [48], although it is expected to have oral bioactivity [44]. MLN9708 is orally available and its efficacy has been demonstrated in phase I clinical trials with oral administration [49]; however, this drug is speculated to be ineffective for MM carrying ß5-subunit mutations because of its boronate-based structure similar to bortezomib. Recently, in contrast to our speculation, Chauhan et al. [50] reported the effectiveness of MLN9708 to overcome bortezomib resistance. As several mechanisms have been proposed for bortezomib resistance in addition to ß5 subunit mutations [51], MLN9708 may be effective for such cases.

HPDs are expected to compensate for the weak points of bortezomib as well as the second generation PIs described above, because HPDs are non-peptide agents that inhibit all three catalytic subunits of the proteasome with equal kinetics and could be orally bioactive. Moreover, crystal structure analyses indicate that the binding mode is completely different from that of bortezomib [39] and NPI-0052 [52]. This ensures the activity of this agent against bortezomib-resistant cells, which was experimentally proven in this study, and probably against cells de-

veloping the resistance to NPI-0052. Moreover, we have found that oral administration of K-7174 is indeed effective and is not associated with obvious toxicities, including leukocytopenia, in a murine xenograft model (manuscript in preparation). These features provide a rationale for the clinical translation of HPDs as novel PIs with effectiveness for the treatment of bortezomib-resistant patients, a low probability of acquired drug resistance, and flexibility in dosing schedules.

Acknowledgments

We are grateful to Dr. Hiroaki Kimura (Jichi Medical University) for helpful discussions and technical advice. We are indebted to Ms. Akiko Yonekura for excellent technical assistance.

Author Contributions

Conceived and designed the experiments: JK NS S-YP YF. Performed the experiments: JK NS SY TW MN KS MO S-YP. Analyzed the data: JK NS S-YP YF. Contributed reagents/materials/analysis tools: TI MA YK. Wrote the paper: JK NS S-YP YF.

References

1. Sawyers C (2004) Targeted cancer therapy. Nature 432: 294–297.
2. Weissman AM, Shabek N, Ciechanover A (2011) The predator becomes the prey: regulating the ubiquitin system by ubiquitination and degradation. Nat Rev Mol Cell Biol 12: 605–620.
3. Frankland-Searby S, Bhaumik SR (2012) The 26S proteasome complex: An attractive target for cancer therapy. Biochem Biophys Acta 1825: 64–76.
4. Richardson PG, Mitsiades C, Schlossman R, Ghobrial I, Hideshima T, et al. (2008) Bortezomib in the front-line treatment of multiple myeloma. Expert Rev Anticancer Ther 8: 1053–1072.
5. Kikuchi J, Wada T, Shimizu R, Izumi T, Akutsu M, et al. (2010) Histone deacetylases are critical targets of bortezomib-induced cytotoxicity in multiple myeloma. Blood 116: 406–417.
6. Mannava S, Zhuang D, Nair JR, Bansal R, Wawrzyniak JK, et al. (2012) KLF9 is a novel transcriptional regulator of bortezomib- and LBH589-induced apoptosis in multiple myeloma cells. Blood 119: 1450–1458.
7. Yanamandra N, Colaco NM, Parquet NA, Buzzeo RW, Boulware D, et al. (2006) Tipifarnib and bortezomib are synergistic and overcome cell adhesion-mediated drug resistance in multiple myeloma and acute myeloid leukemia. Clin Cancer Res 12: 591–599.
8. Noborio-Hatano K, Kikuchi J, Takatoku M, Shimizu R, Wada T, et al. (2009) Bortezomib overcomes cell-adhesion-mediated drug resistance through down-regulation of VLA-4 expression in multiple myeloma. Oncogene 28: 231–242.
9. San Miguel JF, Schlag R, Khuageva NK, Dimopoulos MA, Shpilberg O, et al. (2008) Bortezomib plus melphalan and prednisone for initial treatment of multiple myeloma. New Engl J Med 359: 906–917.
10. Palumbo A, Bringhen S, Rossi D, Cavalli M, Larocca A, et al. (2010) Bortezomib-melphalan-prednisone-thalidomide followed by maintenance with bortezomib-thalidomide compared with bortezomib-melphalan-prednisone for initial treatment of multiple myeloma: A randomized controlled trial. J Clin Oncol 28: 5101–5109.
11. Harrison SJ, Quach H, Link E, Seymour JF, Ritchie DS, et al. (2011) A high rate of durable responses with romidepsin, bortezomib, and dexamethasone in relapsed or refractory multiple myeloma. Blood 118: 6274–6283.
12. Lonial S, Waller EK, Richardson PG, Jagannath S, Orlowski RZ, et al. (2005) Risk factors and kinetics of thrombocytopenia associated with bortezomib for relapsed, refractory multiple myeloma. Blood 106: 3777–3784.
13. Richardson PG, Briemberg H, Jagannath S, Wen PY, Barlogie B, et al. (2006) Frequency, characteristics, and reversibility of peripheral neuropathy during treatment of advanced multiple myeloma with bortezomib. J Clin Oncol 24: 3113–3120.
14. Lu S, Yang J, Song X, Gong S, Zhou H, et al. (2008) Point mutation of the proteasome 5 subunit gene is an important mechanism of bortezomib resistance in bortezomib-selected variants of Jurkat T cell lymphoblastic lymphoma/leukemia line. J Pharmacol Exp Ther 326: 423–431.
15. Oerlemans R, Franke NE, Assaraf YG, Assaraf YG, Cloos J, et al. (2008) Molecular basis of bortezomib resistance: proteasome subunit ß5 (PSMB5) gene mutation and over-expression of PSMB5 protein. Blood 112: 2489–2499.
16. Lu S, Yang J, Chen Z, Gong S, Zhou H, et al. (2009) Different mutants of PSMB5 confer varying bortezomib resistance in T lymphoblastic lymphoma/leukemia cells derived from the Jurkat cell line. Exp Hematol 37: 831–837.
17. Ri M, Iida S, Nakashima T, Miyazaki T, Mori F, et al. (2010) Bortezomib-resistant myeloma cell lines: a role for mutated PSMB5 in preventing the accumulation of unfolded proteins and fatal ER stress. Leukemia 24: 1506–1512.
18. Suzuki E, Demo S, Deu E, Keats J, Arastu-Kapur S, et al. (2011) Molecular mechanisms of bortezomib resistant adenocarcinoma cells. PLoS One 6: e27996.
19. Franke NE, Niewerth D, Assaraf YG, van Meerloo J, Vojtekova K, et al. (2012) Impaired bortezomib binding to mutant ß5 subunit of the proteasome is the underlying basis for bortezomib resistance in leukemia cells. Leukemia 26: 757–768.
20. Kitakaze M, Minamino T, Node K, Takashima S, Funaya H, et al. (1999) Adenosine and cardioprotection in the diseased heart. Jpn Circ J 63: 231–243.
21. Umetani M, Nakao H, Doi T, Iwasaki A, Ohtaka M, et al. (2000) A novel cell adhesion inhibitor, K-7174, reduces the endothelial VCAM-1 induction by inflammatory cytokines, acting through the regulation of GATA. Biochem Biophys Res Commun 272: 370–374.
22. Imagawa S, Nakano Y, Obara N, Suzuki N, Doi T, et al. (2003) A GATA-specific inhibitor (K-7174) rescues anemia induced by IL-1ß, TNF-α, or L-NMMA. FASEB J 17: 1742–1744.
23. Nakano Y, Imagawa S, Matsumoto K, Stockmann C, Obara N, et al. (2004) Oral administration of K-11706 inhibits GATA binding activity, enhances hypoxia-inducible factor 1 binding activity, and restores indicators in an in vivo mouse model of anemia of chronic disease. Blood 104: 4300–4307.
24. Takano Y, Hiramatsu N, Okamura M, Hayakawa K, Shimada T, et al. (2007) Suppression of cytokine response by GATA inhibitor K-7174 via unfolded protein response. Biochem Biophys Res Commun 360: 470–475.
25. Drexler HG, Matsuo Y, MacLeod RA (2003) Persistent use of false myeloma cell lines. Hum Cell 16: 101–105.
26. Uno K, Inukai T, Kayagaki N, Goi K, Sato H, et al. (2003) TNF-related apoptosis-inducing ligand (TRAIL) frequently induces apoptosis in Philadelphia chromosome-positive leukemia cells. Blood 101: 3658–3667.
27. de Leeuw RJ, Davies JJ, Rosenwald A, Bebb G, Gascoyne RD, et al. (2004) Comprehensive whole genome array CGH profiling of mantle cell lymphoma model genomes. Hum Mol Genet 13: 1827–1837.
28. Mitsunaga K, Kikuchi J, Wada T, Furukawa Y (2012) Latexin Regulates the abundance of multiple cellular proteins in hematopoietic stem cells. J Cell Physiol 227: 1138–1147.
29. Meng L, Mohan R, Kwok BH, Elofsson M, Sin N, et al. (1999) Epoxomicin, a potent and selective proteasome inhibitor, exhibits in vivo antiinflammatory activity. Proc Natl Acad Sci USA 96: 10403–10408.
30. Smith DM, Wang Z, Kazi A, Li LH, Chan,TH, et al. (2002) Synthetic analogs of green tea polyphenols as proteasome inhibitors. Mol Med 8: 382–392.
31. Otwinowski Z, Minor W (1997) Processing of X-ray diffraction data collection in oscillation mode. Method Enzymol 276: 307–326.
32. Vagin A, Teplyakov A (2000) An approach to multi-copy search in molecular replacement. Acta Crystallogr D Biol Crystallogr 56: 1622–1624.
33. Adams PD, Grosse-Kunstleve RW, Hung LW, Ioerger TR, McCoy AJ, et al. (2002) PHENIX: building new software for automated crystallographic structure determination. Acta Crystallogr D Biol Crystallogr 58: 1948–1954.
34. Emsley P, Cowtan K (2004) Coot: model-building tools for molecular graphics. Acta Crystallogr D Biol Crystallogr 60: 2126–2132.
35. Davis IW, Murray LW, Richardson JS, Richardson DC (2004) MOLPROBITY: structure validation and all-atom contact analysis for nucleic acids and their complexes. Nucleic Acids Res 32: W615–619, doi:10.1093/nar/gkh398.
36. Kikuchi J, Shimizu R, Wada T, Ando H, Nakamura M, et al. (2007) E2F-6 suppresses growth-associated apoptosis of human hematopoietic progenitor cells by counteracting proapoptotic activity of E2F-1. Stem Cells 25: 2439–2447.
37. Wada T, Kikuchi J, Furukawa Y (2012) Histone deacetylase 1 enhances microRNA processing via deacetylation of DGCR8. EMBO Rep 13: 142–149.
38. Furukawa Y, Vu HA, Akutsu M, Odgerel T, Izumi T, et al. (2007) Divergent cytotoxic effects of PKC412 in combination with conventional antileukemic agents in FLT3 mutation-positive versus-negative leukemia cell lines. Leukemia 21: 1005–1014.
39. Groll M, Berkers CR, Ploegh HL, Ovaa H (2006) Crystal structure of the boronic acid-based proteasome inhibitor bortezomib in complex with the yeast 20 S proteasome. Structure 14: 451–456.
40. De Bettignies G, Coux O (2010) Proteasome inhibitors: Dozens of molecules and still counting. Biochimie 92: 1530–1545.
41. Ruschak AM, Slassi M, Kay LE, Schimmer AD (2011) Novel proteasome inhibitors to overcome bortezomib resistance. J Natl Cancer Inst 103: 1007–1017.
42. Kuhn DJ, Chen Q, Voorhees PM, Strader JS, Shenk KD, et al. (2007) Potent activity of carfilzomib, a novel, irreversible inhibitor of the ubiquitin-proteasome pathway, against preclinical models of multiple myeloma. Blood 110: 3281–3290.
43. O'Connor OA, Stewart AK, Vallone M, Molineaux CJ, Kunkel LA, et al. (2009) A phase I dose escalation study of the safety and pharmacokinetics of the novel proteasome inhibitor carfilzomib (PR-171) in patients with hematological malignancies. Clin Cancer Res 15: 7085–7091.
44. Chauhan D, Catley L, Li G, Podar K, Hideshima T, et al. (2005) A novel orally active proteasome inhibitor induces apoptosis in multiple myeloma cells with mechanisms distinct from Bortezomib. Cancer Cell 8: 407–419.

45. Piva R, Ruggeri B, Williams M, Costa G, Tamagno I, et al. (2008) CEP-18770: A novel, orally active proteasome inhibitor with a tumor-selective pharmacologic profile competitive with bortezomib. Blood 111: 2765–2775.
46. Kupperman E, Lee EC, Cao Y, Bannerman B, Fitzgerald M, et al. (2010) Evaluation of the proteasome inhibitor MLN9708 in preclinical models of human cancer. Cancer Res 70: 1970–1980.
47. Chauhan D, Singh AV, Aujay M, Kirk CJ, Bandi M, et al. (2010) A novel orally active proteasome inhibitor ONX 0912 triggers in vitro and in vivo cytotoxicity in multiple myeloma. Blood 116: 4906–4915.
48. Millward M, Price T, Townsend A, Sweeney C, Spencer A, et al. (2012) Phase 1 clinical trial of the novel proteasome inhibitor marizomib with the histone deacetylase inhibitor vorinostat in patients with melanoma, pancreatic and lung cancer based on in vitro assessments of the combination. Invest New Drugs 30: 2303–2317.
49. Moreau P, Richardson PG, Cavo M, Orlowski RZ, San Miguel JF, et al. (2012) Proteasome inhibitors in multiple myeloma: 10 years later. Blood 120: 947–959.
50. Chauhan D, Tian Z, Zhou B, Kuhn D, Orlowski R, et al. (2011) In vitro and in vivo selective antitumor activity of a novel orally bioavailable proteasome inhibitor MLN9708 against multiple myeloma cells. Clin Cancer Res 17: 5311–5321.
51. Mujtaba T, Dou QP (2011) Advances in the understanding of mechanisms and therapeutic use of bortezomib. Discov Med 12: 471–480.
52. Groll M, Huber R, Potts BC (2006) Crystal structures of salinosporamide A (NPI-0052) and B (NPI-0047) in complex with the 20 S proteasome reveal important consequences of ß-lactone ring opening and a mechanism for irreversible binding. J Am Chem Soc 128: 5136–5141.

PLOS | ONE

Purine Analog-Like Properties of Bendamustine Underlie Rapid Activation of DNA Damage Response and Synergistic Effects with Pyrimidine Analogues in Lymphoid Malignancies

Nobuya Hiraoka[1], Jiro Kikuchi[1], Takahiro Yamauchi[2], Daisuke Koyama[1], Taeko Wada[1], Mitsuyo Uesawa[3], Miyuki Akutsu[3], Shigehisa Mori[4], Yuichi Nakamura[5], Takanori Ueda[2], Yasuhiko Kano[3], Yusuke Furukawa[1]*

1 Division of Stem Cell Regulation, Center for Molecular Medicine, Jichi Medical University, Shimotsuke, Tochigi, Japan, **2** Division of Hematology and Oncology, Faculty of Medical Sciences, University of Fukui, Eiheiji, Fukui, Japan, **3** Department of Hematology, Tochigi Cancer Center, Utsunomiya, Tochigi, Japan, **4** Medical Education Center, Saitama Medical University, Moroyama, Saitama, Japan, **5** Department of Hematology, Saitama Medical University, Moroyama, Saitama, Japan

Abstract

Bendamustine has shown considerable clinical activity against indolent lymphoid malignancies as a single agent or in combination with rituximab, but combination with additional anti-cancer drugs may be required for refractory and/or relapsed cases as well as other intractable tumors. In this study, we attempted to determine suitable anti-cancer drugs to be combined with bendamustine for the treatment of mantle cell lymphoma, diffuse large B-cell lymphoma, aggressive lymphomas and multiple myeloma, all of which are relatively resistant to this drug, and investigated the mechanisms underlying synergism. Isobologram analysis revealed that bendamustine had synergistic effects with alkylating agents (4-hydroperoxy-cyclophosphamide, chlorambucil and melphalan) and pyrimidine analogues (cytosine arabinoside, gemcitabine and decitabine) in HBL-2, B104, Namalwa and U266 cell lines, which represent the above entities respectively. In cell cycle analysis, bendamustine induced late S-phase arrest, which was enhanced by 4-hydroperoxy-cyclophosphamide, and potentiated early S-phase arrest by cytosine arabinoside (Ara-C), followed by a robust increase in the size of sub-G1 fractions. Bendamustine was able to elicit DNA damage response and subsequent apoptosis faster and with shorter exposure than other alkylating agents due to rapid intracellular incorporation via equilibrative nucleoside transporters (ENTs). Furthermore, bendamustine increased the expression of ENT1 at both mRNA and protein levels and enhanced the uptake of Ara-C and subsequent increase in Ara-C triphosphate (Ara-CTP) in HBL-2 cells to an extent comparable with the purine analog fludarabine. These purine analog-like properties of bendamustine may underlie favorable combinations with other alkylators and pyrimidine analogues. Our findings may provide a theoretical basis for the development of more effective bendamustine-based combination therapies.

Citation: Hiraoka N, Kikuchi J, Yamauchi T, Koyama D, Wada T, et al. (2014) Purine Analog-Like Properties of Bendamustine Underlie Rapid Activation of DNA Damage Response and Synergistic Effects with Pyrimidine Analogues in Lymphoid Malignancies. PLoS ONE 9(3): e90675. doi:10.1371/journal.pone.0090675

Editor: Tadayuki Akagi, Kanazawa University, Japan

Received August 8, 2013; **Accepted** February 4, 2014; **Published** March 13, 2014

Funding: This work was supported in part by the High-Tech Research Center Project for Private Universities: Matching Fund Subsidy from MEXT, a Grant-in-Aid for Scientific Research from JSPS (to J.K. and Y.F.), and research grants from Japan Leukemia Research Fund, Takeda Science Foundation (to J.K.), The Naito Foundation, The Yasuda Medical Foundation, and The Uehara Memorial Foundation (to Y.F.). YF received research funding from Eisai Co., Janssen Pharmaceutical K.K., and Novartis Pharmaceuticals Co. N.H. is a winner of the Young Scientist Award of Jichi Medical University. The funders had no role in study design, data collection and analysis, decision to publish, or preparation of the manuscript.

Competing Interests: The authors would like to declare the following: Y.F. received research funding from Eisai Co., Janssen Pharmaceutical K.K., and Novartis Pharmaceuticals Co. This does not alter the authors' adherence to all the PLoS ONE policies on sharing data and materials.

* E-mail: furuyu@jichi.ac.jp

Introduction

Bendamustine, 4-{5-[bis(2-chloroethyl)amino]-1-methyl-2-benzimidazolyl} butyric acid hydrochloride, is a bifunctional alkylating agent synthesized in the 60 s with the aim of combining the alkylating properties of 2-chloroethylamine and the antimetabolite properties of a benzimidazole ring [1]. Bendamustine is believed to act primarily as an alkylating agent that induces interstrand DNA cross-linking and subsequent strand breaks [2], but partial cross-resistance suggests a different mode of action between bendamustine and other alkylating agents such as cyclophosphamide, melphalan and cisplatin [3,4]. Previous studies indicated the activation of DNA damage response and subsequent apoptosis, inhibition of mitotic checkpoints, and induction of mitotic catastrophe as the mechanisms of action of bendamustine [4–7]; however, most of them are shared with other alkylating agents and fail to explain the unique feature of this drug. It is likely that the purine analog-like structure contributes to the uniqueness of bendamustine, but this possibility has not yet been proven.

Bendamustine was used for the treatment of a variety of hematological and non-hematological malignancies between 1971 and 1992 in the German Democratic Republic [1]. Recent clinical trials in Europe and the United States confirmed the efficacy and safety of bendamustine as a single agent for chronic lymphocytic

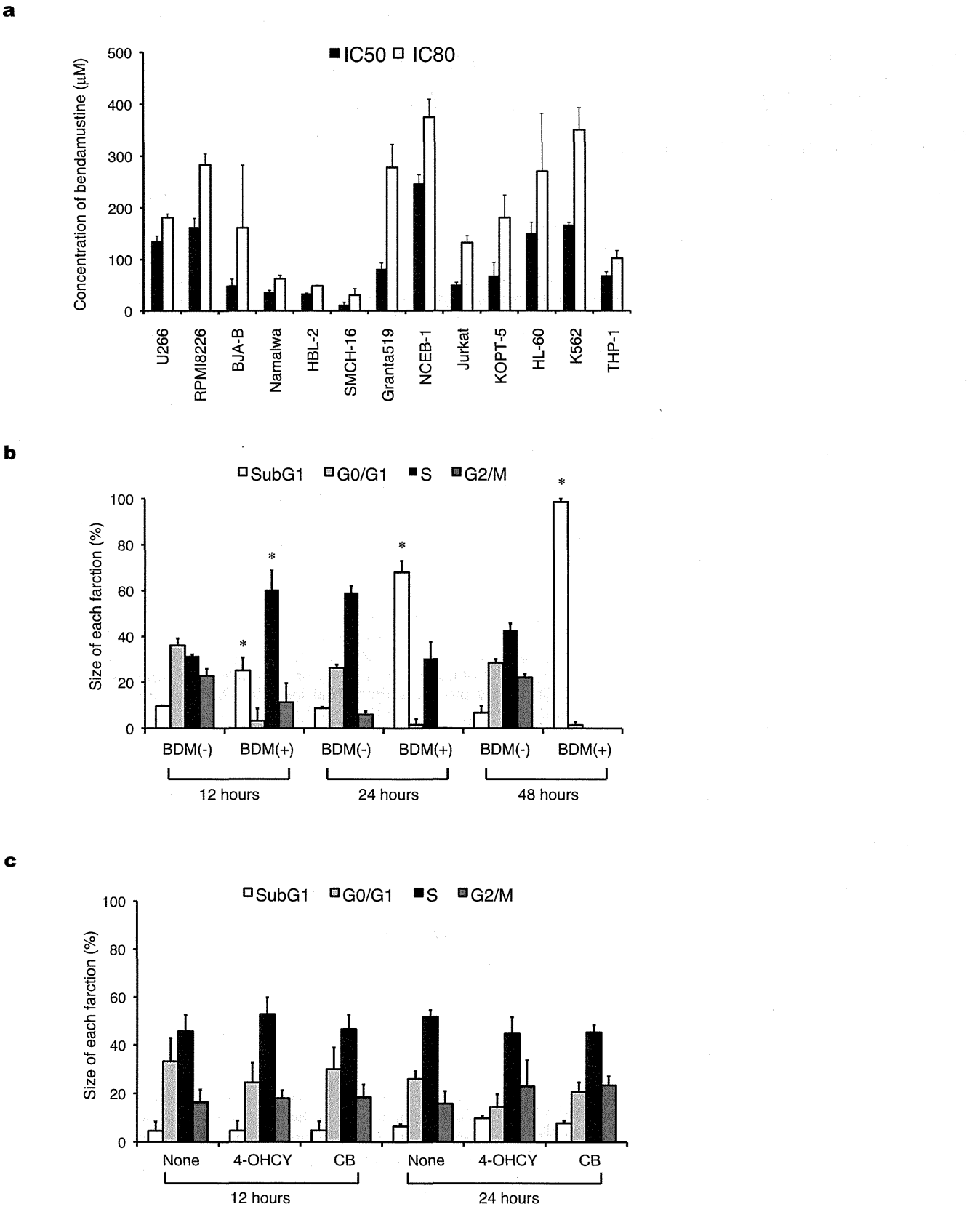

Figure 1. Bendamustine induces apoptosis faster than other alkylating agents but does not exert sufficient cytotoxicity against all tumors. A) We cultured the indicated cell lines with various concentrations of bendamustine and measured cell proliferation with the MTT reduction assay after 72 hours. IC50 and IC80 values are defined as the concentrations of drugs that produce 50 and 80% inhibition of cell growth, respectively. The means ± S.D. (bars) of three independent experiments are shown. B) HBL-2 cells were cultured in the absence (−) or presence (+) of the IC50 value of bendamustine (BDM), harvested at the indicated time points, and stained with propidium iodide in preparation for cell cycle analysis. C) HBL-